

1N7700507

B.A.R.C.-882

B.A.R.C.-882



सत्यमेव जयते

भारत सरकार

GOVERNMENT OF INDIA

परमाणु ऊर्जा आयोग

ATOMIC ENERGY COMMISSION

ANNUAL REPORT
OF THE
METALLURGY DIVISION
Period Ending December 1975

भाभा परमाणु अनुसंधान केन्द्र
BHABHA ATOMIC RESEARCH CENTRE
बंबई, भारत
BOMBAY, INDIA

1976

B.A.R.C.-882

GOVERNMENT OF INDIA
ATOMIC ENERGY COMMISSION

B.A.R.C.-882

ANNUAL REPORT
OF THE
METALLURGY DIVISION
Period Ending December 1975

BHABHA ATOMIC RESEARCH CENTRE
BOMBAY, INDIA
1976

BHABHA ATOMIC RESEARCH CENTRE
METALLURGY DIVISION

ANNUAL REPORT

1975

The Metallurgy Division has been engaged in major programmes on (i) flow-sheet development for the production of rare metals, alloys and special materials of interest to the nuclear programme, electronics and other industry, (ii) physical and mechanical metallurgy of zirconium and titanium alloys, (iii) inter-metallic diffusion and radiation damage studies, (iv) fine particle technology and powder metallurgy, (v) development of nuclear ceramic materials, high alumina compositions and electrical ceramics, (vi) corrosion behaviour of zirconium alloys in high temperature water and selected alloys in sea water systems, and (vii) electro-winning and electro-deposition of metals.

Good progress was maintained during the year on process development relating to a variety of strategic materials including titanium, niobium, tantalum, boron, beryllium, and their alloys. In the Titanium Pilot Plant programme, a major achievement was the commissioning of the 300 mm dia fluidised bed chlorinator - incorporating internal heating through combustion of coke - for the production of $TiCl_4$ at a rate better than 20 kg/hour. (Total production in several campaigns has amounted to about 16 tonnes of $TiCl_4$). For the electrolytic production of titanium metal from $TiCl_4$, employing an alkali chloride fused salt bath, an internally heated, refractory-lined 1000 amp. electrolytic cell has been assembled and successfully tested. Laboratory scale experiments have been successfully carried out on the reclamation of zircaloy and titanium metal scrap by fused salt electro-refining. Flow-sheets have been developed for the preparation of boron-carbide, aluminium-35% boron carbide (boral) sheets to be used as thermal neutron shield, and aluminium-80% boron carbide hollow cylindrical composites as possible shut off rod material for the R-5 reactor. Programmes on the preparation of copper-clad Nb-Ti wires for super-conducting application and of Cu-Be alloys (from

Indian beryl) for the electrical and electronic industry have been continued. The preparation of beryllium metal shapes by hot pressing of beryllium powder is under investigation.

A new Transmission Electron Microscope (capable of 3\AA resolution at 500,000 magnification) and a Scanning Electron Microscope (capable of 100\AA resolution and a maximum magnification of 240,000) were installed and commissioned during the year. The Transmission Microscope is being used for studying phase transformations and precipitation phenomena in zirconium, titanium and tantalum systems, and the Scanning Electron Microscope for studies on failure analysis of power plant components, and fractured zircaloy tubes etc. and characterisation of fine metal powders. Programmes on internal friction measurements in zirconium base alloys to establish interstitial substitutional solute interaction, and inter-diffusion studies in various metal systems using the electron microprobe have been continued. Detailed studies have been undertaken with zircaloy-2 to correlate its thermo-mechanical treatment with the final grain structure and mechanical properties. In the context of the development of Zr-Nb alloys, a consumable electrode arc furnace assembly, with electrode feed and power control is under commissioning. A freeze drying unit has been designed and commissioned for the preparation of ultrafine particles of metal compounds for further conversion to fine metal powders required in the preparation of porous metal components of controlled porosity. A study on the generation of helium bubbles on neutron irradiation of copper-boron alloys has been completed.

The corrosion behaviour of several potentially interesting zirconium base alloys in high temperature water and steam has been studied and compared with that of zircaloy-2. A programme has been initiated to study in detail the stress corrosion cracking behaviour of zircaloy fuel tubing. Extensive corrosion testing has been carried out with aluminium base alloys, copper-base alloys, cupro-nickels, stainless steel and cast iron in saline media in order to select materials for service in desalination plants and sea water cooling systems. In the electro-

metallurgy programme, work is in progress on the preparation of individual rare earth metals and cobalt rare earth magnet alloys by fused salt electrolysis and on the electro-deposition of copper-alumina, nickel-alumina and nickel-titania composites.

A comprehensive investigation has been undertaken to establish a reliable and reproducible correlation between uranium oxide powder production practice, powder characteristics and sintering behaviour. This programme would also include a critical assessment of the influence of morphology, crystallinity and surface activity of the UO_2 powder on its sintering behaviour. Flash-heating of UO_2 powders and densification of sintered UO_2 pellets on refiring at higher temperature are other aspects under study.

It has been possible to prepare and fabricate high purity single phase barium titanate compacts of very high dielectric constant and low dissipation factor, starting with barium titanate powder obtained from barium titanyl oxalate. Development programmes on high density high alumina bodies and impervious mullite for industrial applications, and basic research programmes on the sintering behaviour of magnesium oxide and beryllium oxide have been continued.

C.V. Sundaram
Head, Metallurgy Division

1. EXTRACTIVE METALLURGY

Good progress was maintained during the year on process development programmes - on bench scale and pilot plant scale - for various strategic materials. Major programmes have related to beryllium and copper-beryllium, niobium-based superconducting alloys, boron carbide and electrolytic titanium. Special emphasis has been laid on metallo-thermic and carbo-thermic reduction, vacuum metallurgy, and fused salt electrolysis. Basic research on metallurgical thermo-chemistry has been continued and expanded.

1.1 INDUSTRIAL PROJECTS

1.1.1 Titanium Pilot Plant

The Titanium Pilot Plant (7.5 tonnes/year of Ti-sponge) at the Nuclear Fuel Complex (NFC), Hyderabad was in regular operation during the year.

In the fluidised bed chlorination of rutile-carbon mixtures, it has been found that if instead of electrical heating the bed is heated by the internal combustion of coke with oxygen, the operation becomes much more smooth and trouble-free. A larger chlorinator (300 mm dia) heated internally with coke-oxygen has been successfully designed and operated to produce $TiCl_4$ at the rate of 450 kgs/hr/m². In this chlorinator with a bed height of 650 mm (particle size 100 micron), when the chlorination has been carried out at 900-1050°C, the chlorine utilisation and rutile utilisation efficiencies have been found to be of the order of 80-90% and 90-95% respectively. A total of 16 tonnes of $TiCl_4$ was produced in several campaigns.

In the production of titanium metal by the magnesium reduction of $TiCl_4$, the system has been suitably modified for effective tapping of by-product magnesium chloride. From the metal produced in the pilot plant, supplies have been made to various organisations in the country.

1.1.2 Beryllium Alloy and Metal Plant

Based on specific requirements of beryllium metal and copper-beryllium alloy indicated by the Departments of Space and Electronics, a revised project report for the setting up of a Beryllium Alloy and Metal Plant (10 T/year of Cu-2% Be alloy and 250 kg/year of hot pressed beryllium metal) has been prepared. The capital outlay for the proposed plant has been estimated at Rs.54.4 lakhs (P.E. component of only Rs.4.47 lakhs).

1.1.3 Niobium Plant

A revised project report for the setting up of a Niobium Plant (3 T/year) as an annexe to the Special Materials Plant, NFC, Hyderabad has been prepared. The capital outlay is estimated at Rs.36.25 lakhs (P.E. component of only Rs.3.53 lakhs).

1.2 PRODUCTION AND FABRICATION OF BORON CARBIDE

(C.K. Gupta, D.K. Bose, A.K. Suri, P.V.S. Pillai and K.U. Nair)

Natural boron and its compounds by virtue of their B^{10} content (18.8% of total boron) find application as neutron shields (neutron absorption cross section $\sigma = 750$ barns) and control rods in nuclear reactors and nuclear devices. Amongst the various boron compounds boron carbide (B_4C - 78.3% boron) is the most suitable neutron absorber material, considering both layer thickness and cost. The carbide is not only cheaper than elemental boron by several orders of magnitude but it has higher temperature and abrasion resistance and chemical inertness and excellent radiation stability.

A preliminary survey at Trombay has indicated a definite demand for boron carbide composites and boron (a cermet composed of B_4C and Al) in nuclear reactor programmes.

1.2.1 Carbothermic Reduction Process for Boron Carbide Production

Investigations on the production of B_4C powder have been continued and the optimum conditions and procedure for the carbothermic reduction of boric oxide in an induction furnace have been established. In a typical run 575 g of anhydrous B_2O_3 (dried under vacuum at $150^\circ C$) has been reacted with 300 g of activated charcoal in a graphite crucible in an induction furnace at a temperature above $2000^\circ C$ (power level of 14.5 KW) for about 4 hrs. About 160 g of boron carbide/batch at a recovery of 80% could be prepared by this method. A minor addition of K_2CO_3 as a catalyst (5% by wt. of the charge) helps in bringing down the reaction time to 2 hrs and improves the carbide yield by about 10%.

1.2.2 Production of Boron Carbide by Magnesiothermic Reduction of B_2O_3 in Presence of Carbon

Development work on the production of B_4C by magnesiothermic reduction has also been undertaken besides regular production by carbothermic reduction. A number of experiments with charge composing of B_2O_3 , Mg, carbon and NaCl/MgO (as heat diluent) have been carried out with and without the addition of catalyst (potassium sulphate). In the presence of the catalyst the reaction takes place at around $680^\circ C$, otherwise a temperature of as high as $900^\circ C$ is required. The reacted mass is leached with water and then with 60% H_2SO_4 to remove MgO, unreacted B_2O_3 and Mg. The product has been found to be predominantly B_4C on X-ray analysis.

1.2.3 Fabrication of Boral Sheets and Boron-carbide - aluminium Hollow Cylindrical Compacts

Boral, a dispersion of B_4C in aluminium, is a well established thermal neutron shield material. The process for the production of boral (35 wt % B_4C , balance Al) in the finished sheet form has been standardised in the laboratory. The procedure involves the following three steps : (i) preparation of boral cast, (ii) picture framing

and cladding of the cast with aluminium and (iii) hot rolling of the clad cast. In the preparation of boron cast, preoxidised B_4C (at $900^\circ C$ for 1 hr.) is intimately mixed with aluminium powder (-100 +200 mesh) and charged directly in a graphite mould (150 x 200 x 30 mm) and heated in a pit furnace, and at $700^\circ C$ the charge is mixed in a paddle type mixer. Wettability of aluminium under this condition is satisfactory and after 15 minutes of mixing it has been possible to obtain a homogeneous pasty mass. Finally the top surface of the cast is pressed with a mandrel to obtain 150 x 200 x 25 mm boron slab. The cast is then picture framed with 6 mm thick aluminium plate and then clad with 3 mm thick aluminium sheet. The assembly was heated to $610^\circ C$, soaked for an hour and then rolled allowing 10% reduction per pass. Immediate soaking after almost every pass was necessary to maintain the working temperature at about $600^\circ C$. Hot rolled sheet (6 - 10 mm) fabricated by this procedure has good surface finish and bonding between the aluminium cladding and the boron sandwich.

Investigations were carried out on the preparation of aluminium bonded hollow cylindrical boron carbide (B_4C) shapes for possible use as sheet rod in research and power reactors. Both cold compacting and sintering and hot pressing technique have been examined for the fabrication of 62 mm O.D., 46 mm I.D., 20-22 mm height hollow cylindrical ring containing 80% B_4C and 20% Al. Product obtained by hot pressing was found to be superior in surface finish and density. In the hot pressing technique, the influence of experimental parameters such as temperature (600-780°C), compacting pressure (1000-1700 psi) and time (15-60 min) on quality of the sintered product has been investigated. Hot pressing at a temperature of 680°C and 1700 psi pressure for 45 min. appeared to be optimum for fabricating rings of the dimension mentioned above.

1.3 SUPER-CONDUCTING ALLOYS
(D.K. Bose, C. Narayanan and C.K. Gupta)

1.3.1 Fabrication of Nb-Ti Super-conducting Alloys

Amongst all superconducting alloys, Nb-Ti has assumed greatest commercial importance owing to its easy fabricability, low cost and superior electrical properties (current carrying capacity 10^5 A/cm² at 120 KG). A programme initiated earlier in the Section to generate know-how on the preparation and fabrication of Nb-Ti superconductors has been continued during the year. The procedure for the preparation of Nb-40-50% Ti alloy consists of the following steps : (i) electron beam melting of nuclear grade Nb and high purity Ti, (ii) homogenisation of the cast at 1500°C for 2-5 hrs., (iii) β -quenching (for 800°C) of the sample, (iv) rolling in a 20 stage grooved rolling mill to 1.2 mm dia wire rod, (v) intermediate annealing at 1000°C for 2 hrs. under vacuum, (vi) progressive drawing through tungsten carbide dies to 0.5 mm ϕ wire, and (vii) cleaning, pickling and encapsulation in a silica tube, and final heat treatment at 350°C for 1 hr followed by water quenching. An evaluation test performed on the wire (0.5 mm ϕ) indicated that the wire can carry currents of 48 A, 43 A and 20 A, at 4.2°K, under magnetic fields of 7.5 KOe, 12 KOe and 24 KOe respectively.

1.3.2 Preparation of Nb-Zr and Nb-Ti Alloys by
Co-reduction of the Metal Oxides

A programme has been initiated on the production of Nb-Zr and Nb-Ti alloy powders by Co-reduction of mixed oxides with calcium hydride. The process is quite attractive as by this it is possible to produce a homogeneous alloy powder suitable for making superconducting material. In addition Nb-50% Zr alloy powder which can be produced by this method can be used as a master alloy for subsequent dilution to Zr-2.5% Nb.

The procedure adopted for the preparation of the alloy powder involved (i) reduction of mixed oxides with CaH at 1000-1150°C under vacuum, (ii) acid leaching of the reacted mass to isolate alloy powder

from Ca and CaO, (iii) vacuum drying of the product, (iv) vacuum sintering of the powder compact at 1200-1650°C to remove volatile impurities, (v) arc or electron beam melting of sintered product. The Nb-50% Zr alloy prepared by this method indicated a button hardness of as low as 408 VHN as against 330 VHN for similar alloy prepared by direct melting. Further work on achieving higher purities by careful control of process parameters is in progress.

1.4 ZIRCONIUM/HAFNIUM TECHNOLOGY

1.4.1 Soda Ash Sintering of Zircon

(T.S. Krishnan, J.M. Juneja and P.R. Menon)

The development of an alternate route for the economic production of commercial grade ZrO_2 starting from Indian zircon, involving preferential solubilisation of silica by lime stone/dolomite sintering of the ore followed by aqueous processing has been studied and the results reported earlier. The process is being examined for its suitability for commercial exploitation.

The lime sintering process as described above, though found suitable for production of commercial grade ZrO_2 , cannot however be employed for the preparation of zirconium compounds and for high purity zirconium oxide. Alkali fusion is widely employed for the opening up of zircon at present and in this process both zirconia and silica values in zircon are solubilised. In view of this, the raw material and operational costs are substantially high reflecting ultimately in the cost of the oxide and the compound produced by this method. R & D work was therefore initiated to examine the possibility of substituting caustic soda by soda ash in the charge. Experiments have been carried out using -325 mesh zircon with different proportions of sodium carbonate and it has been observed that when a charge containing zircon and sodium carbonate in the mole ratio 1 : 1.1 is sintered at 1050°C for 1 hr and subsequently leached with acid an oxide having a purity of better than 99.5% is obtained at a recovery of

about 90%. The major attraction of this process lies in the selectivity of the reaction between zircon and sodium carbonate when the carbonate is present upto a certain proportion. During sintering the carbonate reacts preferentially with zirconium oxide and the unreacted silica gets separated in the course of acid leaching. Zirconium hydroxide is then precipitated from the acidic solution by addition of ammonium hydroxide and finally calcined at 800°C to obtain zirconium oxide. The selective nature of the reaction considerably reduces the raw material requirements; thus resulting in a substantial reduction in the manufacturing cost.

Further work to improve the oxide recovery and also on the scale up of operation is in progress.

1.4.2 Reclamation of Zirconium from Scrap by Fused Salt Electrolysis

(J.C. Sehra, P.L. Vijay and I.G. Sharma)

Studies on the recovery of zirconium from zircaloy scrap by fused salt electrolysis have been successfully completed during the year. The process as developed here essentially consists in the electrolysis of zircaloy scrap (anode feed) charged at the bottom of a graphite crucible in the cell assembly using $\text{NaCl-K}_2\text{ZrF}_6$ bath. The electrolytic cell consists of a 150 mm I.D. inconel retort with a receiver lock at the top and facilities for evacuation, argon purging and cathode placement. A slide valve isolates the cathode chamber from the anode. A graphite crucible placed inside the retort serves both as anode and anode feed container. A molybdenum strip attached to a stainless steel rod forms the cathode.

The system is first evacuated and after ensuring leak tightness is back filled with argon and heated to the desired temperature. Pre-electrolysis is then carried out at a lower current density to remove moisture and other undesirable impurities prior to electrodeposition of zirconium. The influence of parameters such as percentage of soluble

zirconium in the bath, (2, 5, 10, 12.5 and 15%) temperature of electrolysis - 800, 850, 900 and 950°C - and current density (15.6, 21.4, 25.8, 32.2 and 43.0 Am/dm²) on the yield and purity of the metal has been studied. Under the optimised conditions zirconium could be deposited at a current efficiency of 70% at a c.c.d. of 25.8 Amp/dm² at 850°C from a bath containing 10 wt% soluble zirconium. The metal when arc melted has given a button hardness of 140-160 BHN compared to 330 BHN for the scrap.

1.4.3 Graphite Lubrication on Zircaloy Tubing (C.K. Gupta and T.K. Mukherjee)

Some of the failures of zircaloy-2 tubes used as sheath for fuel in the thermal reactors have been traced to stress corrosion cracking resulting from fuel sheath interaction. Investigations have been taken up to examine the possibility of reducing this interaction and hence the failure, by using graphite as lubricant. The application of the lubricant on the tube interior is achieved by giving a thin graphite coat of about 10 micron thickness by contacting with Poliac-20 for about 2 minutes. The tube is then air dried for 24 hrs. and hardened by vacuum baking at 300°C for 2 hrs. Evaluation of the graphite film for its adherence is in progress.

1.4.4 Electrowinning of Hafnium Metal (J.C. Sehra, P.L. Vijay and I.G. Sharma)

Work on the direct electro-winning of hafnium metal by fused salt electrolysis of HfCl₄ was continued during the year. An inconel electrolytic cell (203 mm I.D., 800 mm length and 6 mm wall thickness) with properly separated anode and cathode ports has been fabricated. The isolation of the anode port will facilitate fast and effective removal of the liberated chlorine; thus minimising corrosion. The cathode port provides a receiver lock which helps in the removal of electrodeposited metal and insertion of a fresh cathode.

1.5 TITANIUM DEVELOPMENT PROGRAMME

(H.S. Ahluwalia*, A.P. Kulkarni*, Ch. Sridhar Rao & C.V. Sundaram)

Of the three major methods for the production of titanium metal namely (1) magnesium reduction of $TiCl_4$, (2) sodium reduction of $TiCl_4$, and (3) fused salt electrolysis of $TiCl_4$, the first two have already been standardised and are successfully being employed in the Titanium Pilot Plant at NFC, Hyderabad. The electrolytic route is being investigated at Trombay. During the year, the developmental work on the fused salt electrolysis of $TiCl_4$ was continued.

1.5.1 Chlorination of Rutile

(Ch. Sridhar Rao and P.L. Vijay)

Detailed investigations have been carried out on the chlorination of rutile and the influence of various parameters such as temperature, particle size of rutile, coke-rutile ratio and bed height on chlorination rate and chlorine utilisation efficiency has been studied. It has been observed that while the chlorination rate depends on the rutile particle size, chlorination temperature and coke-rutile ratio, the chlorine utilisation is directly proportional to the bed height.

1.5.2 Electrolysis of $TiCl_4$

(Ch. Sridhar Rao, T.K. Mukherjee, C. Subramanian & K. Swaminathan)

The cell assembly set up earlier for the fused salt electrolysis of $TiCl_4$ has been suitably modified for smooth and efficient operation. The electrolytic cell consists essentially of a rectangular mild steel chamber lined with acid resistant refractory bricks. Two 80 mm wide, 3 mm thick and 200 mm long inconel strips have been found more suitable for heating the bath as compared to the coil and rod heaters used earlier. The two rectangular graphite anodes have been found to give a better and longer service when their thickness was increased from 50 to 100 mm. The cathode consists of a perforated nickel basket attached to an inconel tube.

(*) Nuclear Fuel Complex, Hyderabad.

The corrosion of the cathode pipe could be minimized to a large extent by giving a cement coat over the pipe. There is an upper chamber over the electrolyte bath which is isolated with a water cooled slide valve. The upper chamber wherein also an argon atmosphere is maintained helps in holding the cathode basket containing the deposit till it is cooled to room temperature.

The experimental procedure consists essentially of the following steps. Oven dried KCl-NaCl (1 : 1 wt ratio) after melting in an inconel retort is transferred to the pre-dried cell assembly to build a molten salt height of about 20". The salt as such is then subjected to a pre-electrolysis for a few hours at about 3 volts and 100-250 Amps using a mild steel plate cathode for the removal of moisture and metallic impurities. The electrolysis is then carried out with the nickel basket cathode instead of the mild steel plate cathode, feeding the $TiCl_4$ at the required rate and adjusting the voltage and current in the range of 6-7 volts and 600-700 amps respectively. When the cathode basket gets filled with the deposit it is lifted and placed in the chamber for cooling and an empty cathode basket is simultaneously inserted in place to continue the electrolysis. The cathode deposits after cooling to room temperature are separated from the baskets and washed first with water and then with dilute hydrochloric acid to remove the adherent salts and finally rinsed in acetone and dried at room temperature. The dried metal is finally sieved, graded and packed. The coarser fraction of the electron beam melted metal indicated a button hardness of 160 BHN. The influence of various parameters such as cathode current density, current to feed ratio, voltage and temperature on the electrodeposition of titanium has been studied in detail and the results are given in Table-I. A product recovery of as high as 88% could be achieved at a cathode current efficiency of 55%. Further work to improve the efficiency of the process and the recovery and purity of the product is in progress.

TABLE I
EXPERIMENTAL CONDITIONS AND RESULTS ON THE FUSED
SALT ELECTROLYSIS OF $TiCl_4$

Rate of $TiCl_4$ addition kg/hr	Operating Tempera- ture °C	Voltage volts	Current Amps	c.c.d. Amp/ ft ²	Current/ Feed F/mole	Current Effi- ciency %	Yield %
0.56	790-800	6-7	700	414	8.94	27	59
0.50	830-880	6.5-7	700	414	8.51	31	76
1.363	860	6.5-7	650-700	390	3.51	42	37
0.78	860-870	6-6.25	650-700	414	6.15	46	71
0.78	860	6.5	700	414	6.38	55	88
0.78	800-820	6.5-8	600	360	5.50	60	83

1.5.3 Reclamation of Titanium from Scrap
by Fused Salt Electrolysis
(J.C. Sehra, P.L. Vijay and I.G. Sharma)

Work on the reclamation of titanium from titanium scrap by molten salt electrolysis has been initiated. While the cell and the procedure employed are essentially the same as described for the processing of zirconium scrap, in this case a master mix of the composition $2NaCl \cdot TiCl_2$ prepared by sodium reduction of $TiCl_4$ is used as the electrolytic bath. The master mix is diluted with $NaCl$ to correspond to 57% soluble titanium and the electrolysis carried out using compacted titanium scrap turnings as anode feed with molybdenum as cathode.

In preliminary experiment titanium metal (40-45 mm size) has been deposited at a c.c.d. of 73 Amp/dm^2 ; the cathode current efficiency being 62%. The metal on arc melting gave a button hardness of 100 BHN. Further work is in progress.

1.6 PREPARATION OF THORIUM METAL SPONGE

(J.C. Sehra, P.L. Vijay and C.V. Sundaram)

Preparation of thorium metal sponge by the magnesiothermic reduction of thorium chloride was continued. Thorium chloride has been prepared by the chlorination of thorium oxalate. The chloride after purification is reduced with magnesium to obtain thorium-magnesium alloy which is pyrovacuum processed to obtain thorium metal sponge. The metal sponge has been finally consolidated by electron beam melting.

The suitability of various chlorinating agents such as CO-Cl_2 , $\text{COCl}_4\text{-Cl}_2$ and $\text{CCl}_4\text{-CO}_2$ for the chlorination of thorium oxalate has been investigated in detail on a scale of 300 gms of contained Th. $\text{COCl}_4\text{-Cl}_2$ mixture has been found to be the most suitable chlorinating agent giving a conversion efficiency of 98% and a chlorine utilisation efficiency of 25%. The chloride has been purified by sublimation in a nickel assembly at $750\text{-}800^\circ\text{C}$ and 750 mm pressure.

Pure ThCl_4 has been reduced with magnesium (100% excess over the stoichiometric requirement) in a tantalum crucible at 960°C and at a positive argon pressure of 10 cm of Hg to give a Th-20% Mg alloy. After reduction, the temperature is finally raised to 1050°C and held for half an hour to effect slag-metal separation. After cooling to room temperature Th-Mg alloy is removed from the tantalum crucible and subjected to a pyrovacuum treatment at 900°C and 0.06 micron vacuum to separate the excess Mg and volatile impurities and obtain thorium metal sponge. The metal sponge obtained analyses 850 ppm oxygen, 53 ppm nitrogen, 180 ppm carbon, 0.014% Fe, and 0.014% Mg, and indicates a button hardness of 60 VHN after electron beam melting.

1.7 VANADIUM TECHNOLOGY

(C.K. Gupta and O.K. Mehra)

The flow sheet on the recovery of vanadium from vanadium sludge (obtained as a by-product in the extraction of aluminium by Bayer's process) has been investigated in detail and found suitable for commercial exploitation. The raw material (vanadium sludge containing about 15% V_2O_5) required for the investigations has been procured from M/s Hindustan Aluminium Corporation. Starting from the sludge the productions of calcium vanadium complex, vanadium pentoxide, ferro-vanadium and vanadium metal have been successfully demonstrated.

1.7.1 Recovery of Vanadium from Vanadium Sludge

The flow-sheet for the recovery of vanadium from vanadium sludge in the form of calcium vanadium complex involves (i) treatment of the sludge with Na_2CO_3 solution at 90°C under agitation followed by filtration of the sodium vanadate leach liquor, and (ii) precipitation of vanadium as $CaO.V_2O_5$ by $CaCl_2$ addition at pH 7-8 or as $4 CaO.V_2O_5$ by lime addition at pH-13. Vanadium recovery of as high as 95% has been achievable by this method.

The flow-sheet for the recovery of vanadium pentoxide involves (i) treatment of sludge at 90°C with Na_2CO_3 to obtain sodium vanadate solution and (ii) addition of $NaClO_3$ to the vanadium laden solution to convert tri-valent vanadium to penta-valent state and adjustment of pH at 2-3, (iii) boiling of the vanadate solution to precipitate red cake, (iv) re-dissolution of the red cake in 8% Na_2CO_3 solution, (v) addition of ammonium chloride to precipitate ammonium meta-vanadate, and (vi) decomposition of meta-vanadate at 400-450°C to produce pure V_2O_5 . Vanadium recovery by this procedure was more than 96%.

1.7.2 Aluminothermic reduction of V_2O_5 to produce V, V-Al and Ferro-vanadium

Preparative methods were standardised in this laboratory for the

production of ferro-vanadium/crude vanadium by aluminothermic reduction of V_2O_5 in presence of lime. In this smelting technique lime acts as a heat sink and also forms a low melting slag with alumina which helps in better slag/metal separation. Since lime is present in calcium vanadate this vanadium salt can be used as such in aluminothermic smelting. Starting from both the di- and tetra-calcium complexes of vanadium, process conditions have been optimised for the production of 50 : 50 grade ferro-vanadium.

1.8 BERYLLIUM DEVELOPMENT PROGRAMME
(C.M. Paul and C.V. Sundaram)

The various steps in the flow-sheet for the production of Be-metal and Cu-Be alloys have been investigated in detail to generate more reliable and dependable data required for the design of a large scale production plant. Work has also been initiated to scale up the preparation of the metal, the metal powder and the alloys. In this connection a larger induction furnace (25 KW) capable of melting about 20 kgs of the alloy has been procured, installed and is being commissioned. Action has also been initiated to ventilate and equip one more room of about 400 sq.ft. floor area mainly for the production and handling of beryllium powder. The room will locate (i) a lathe for the production of Be-chips from vacuum induction melted Be-ingots, (ii) a ball mill for further conversion of the chips to powder, (iii) a classifier to separate the coarse powder from the -200 mesh product and (iv) facilities such as glove boxes and special fumehoods for the handling of Be-powder.

Based on the specific requirements of Cu-Be alloy shapes by the Department of Electronics and of Be-metal by the Department of Space, a revised project report for a plant to produce 10 tonnes/year of Cu-2% Be alloys and about 250 kgs/year of Be-metal shapes have been prepared. The capital outlay of the proposed plant has been estimated at Rs.54.4 lakhs with a foreign exchange component of only Rs.4.47 lakhs. Developmental work on the large scale fabrication of Cu-2% Be alloy foils in various

temper states taken up in collaboration with M/s Indian Smelting and Refining Co. is in progress. Besides, limited quantities of various Cu-Be alloy shapes have been produced in the laboratory and supplied to various organisations in the country in response to their urgent requirements.

1.8.1 Preparation of $\text{Be}(\text{OH})_2$ / BeO from Indian Beryl
(K.S. Subbarao, R.H. Rakhasia and C.M. Paul)

Work on the preparation of $\text{BeO}/\text{Be}(\text{OH})_2$ by the silicofluoride sintering of beryl followed by aqueous leaching of the sinter and precipitation of $\text{Be}(\text{OH})_2$ by alkali treatment of aqueous Na_2BeF_4 solution was continued. A method has already been standardised in the Section for the conversion of the Be-values of Indian beryl into water soluble Na_2BeF_4 by sintering a charge containing ground beryl (-200 mesh) and sodium silicofluoride and sodium carbonate (11.15 : 8.1 : 0.95) at 700°C for 4 hrs. Further work has shown the possibility of substituting sodium silicofluoride with sodium ferric fluoride (iron cryolite) almost to the extent of 60% without any reduction in the extraction efficiency. The above modification of the process is of prime importance in the metallurgy of beryllium as this opens up a possibility for recycling the by-product fluorine values as iron cryolite in the process. Attempts have therefore been made to recover fluorine from the aqueous NaF filtrate solution (generated in the precipitation of $\text{Be}(\text{OH})_2$) in the form of iron cryolite by treatment with a ferric salt solution at a pH of 4. The iron cryolite thus obtained is dried and used in the sintering of beryl. By replacing about 60% of the Na_2SiF_6 in the charge mixture with Na_3FeF_6 , when sinterings were carried out at 750°C for 2 hrs. on a scale of 300 gms of contained BeO , the Be-recoveries have been found to be of the order of 90-92%.

1.8.2 Preparation of Anhydrous BeF_2
(B.P. Sharma, K.S. Subbarao, K. Mammadu and C.M. Paul)

Preparation of anhydrous BeF_2 by the thermal decomposition of

$(\text{NH}_4)_2\text{BeF}_4$ - obtainable by the NH_4HF_2 treatment of $\text{Be}(\text{OH})_2$ - is a difficult step in the flow-sheet for the metallurgy of beryllium. The major difficulties being (i) excessive frothing of the double fluoride during decomposition and (ii) tendency for the condensation of the decomposition by-product (NH_4F) also at places other than in the condenser resulting in chocking of lines.

The inclined graphite decomposition assembly designed earlier has been suitably modified and it has been possible to continuously decompose $(\text{NH}_4)_2\text{BeF}_4$ to give anhydrous BeF_2 at the rate of 500 gms/hr. The chocking of the feeder line has been almost completely eliminated by proper drying of the double fluoride and controlling its particle size around 12 mesh. The graphite tube decomposition assembly is held at an angle of 30° to the horizontal and resistance heated with a split furnace to maintain a temperature of 950°C at the discharge end and 750°C at the feed end of the tube. With this arrangement continuous decomposition of the double fluoride has been possible and the molten BeF_2 which flowed down the gradient has been cast in cold graphite moulds.

1.8.3 Preparation of Beryllium and its Alloys from Beryllium Fluoride

(B.P. Sharma, S. Adhikari, M.G. Rajadhyaksha and C.M. Paul)

Work on the preparation of Cu-Be master alloys by the Mg-reduction of BeF_2 in presence of copper at temperatures in the range of 1100 - 1400°C in graphite crucible in induction furnace has been continued on a $\frac{1}{2}$ kg scale of the alloy and the influence of various process parameters such as excess BeF_2 in the charge, Be-loading in the alloy, reduction temperature etc. studied. Dilution of the master alloys to Cu-2% Be alloys has also been carried out successfully on a 2-kg scale in induction furnace. The diluted alloys have been cast to suitable shapes and fabricated to rods and foils by employing techniques like extrusion and rolling.

Investigations have also been continued on the preparation of Be-metal pebbles on a 50-gm scale of the metal by the Mg-reduction of BeF_2 .

The influence of excess BeF_2 on Be-recovery has been studied in detail and it has been observed that a beryllium metal recovery of as high as 80% could be achieved when the BeF_2 excess in the charge has been 40%. The metal pebbles obtained indicated a purity of about 97%.

1.8.4 Hot Pressing of Beryllium Powder
(K.S. Subbarao, R.H. Rakhasia and G.M. Paul)

Beryllium shapes directly fabricated from cast ingots by conventional techniques are unsuitable for commercial applications on account of their brittle nature and poor mechanical properties. Powder metallurgical techniques are therefore generally employed for the fabrication of beryllium shapes. Of the two most common powder metallurgical fabrication methods namely (i) cold compaction and sintering, and (ii) vacuum hot pressing, the latter method is preferred in the case of beryllium for obtaining shapes of higher densities (almost theoretical).

A programme has therefore been initiated on the fabrication of Be-shapes by vacuum hot pressing of Be-powder. An induction heated assembly for the vacuum hot pressing of Be-shapes has been designed, fabricated, installed and commissioned in the laboratory. The assembly consists essentially of a vacuum chamber which accommodates a die and plunger made of high density graphite. The vacuum chamber is fabricated out of 7" dia silica tube closed at both ends with brass flanges. The top flange carries a Wilson seal for the plunger rod and the bottom flange has provisions for connections to an evacuation system which consists essentially of a rotary mechanical pump to give a vacuum of the order of 100 microns. The system has been used to study the influence of various parameters such as compaction pressure, size distribution of the powder and atmosphere of compaction on the final density of the compact. It has been observed that the compaction pressure and temperature can be brought down considerably by selecting a proper size distribution for the powder. For a powder having a definite size distribution

the compacting pressure decreases with increase in temperature. It has also been observed that the densification follows the conventional pattern - the density increasing rapidly initially and slowly in the final stages for a constant compacting temperature.

It has been found that compared to a single stage compaction at the final temperature and pressure a pre-compaction at a lower pressure and temperature followed by compaction at the final temperature and pressure can give pellets having higher densities. Densities as high as 99.8% of the theoretical could be achieved by pre-compacting the powder at 600°C and 1000 psi, gradually increasing the temperature to 1100°C and compacting the same at this temperature at a final pressure of 2000 psi. Densification was found to take place in 3 stages, 1/3rd taking place during pre-compaction, 1/3rd during the subsequent heating period and the remaining 1/3rd during final compaction. In the vacuum hot pressing of 12.5 mm dia pellets, the beryllium losses have been only 1-1.5% as against 25-30% in the case of cold compaction followed by vacuum sintering.

Work on the setting up of a similar system for the fabrication of larger shapes (4" x 4" x 4" compacts) has also been initiated.

1.9 CARBOTHERMIC TECHNOLOGY

1.9.1 Preparation of vanadium oxy-carbide (D.K. Bose and C.K. Gupta)

Like ferro-vanadium and vanadium carbide (V_2C), vanadium oxy-carbide (VO_xCy) is also a proven material suitable for steel addition. The compound (VO_xCy) can easily be formed by carbothermic reduction of V_2O_3 at 1350°C under vacuum. In small scale experiments, 100 g V_2O_3 (hydrogen reduced), required amount of petroleum coke powder (-325 mesh), 4% starch and 10% water are thoroughly mixed and then pelletised. Pellets are then dried in an oven and finally subjected to a vacuum thermal reduction at 1350°C till the vacuum level improved to 100 μ . The ratio of combined

and free carbon to oxygen (y/x) in this product is controlled by controlling carbon content in the charge. In general y/x ratio is maintained between 1.0 to 1.5 for steel addition.

In studies on vanadium additions in the form of vanadium oxy-carbide (VO_xCy , $y/x = 1.25$, 75% V, 5% C), vanadium carbide (V_2C , 90% V, 6.1% C) and ferro-vanadium (Fe-V, 53% V, 1.8% C) to a low carbon steel (0.31% V, 0.1% C) it has been observed that the carbon contents of the steel melts have been 0.9%, 0.16% and 0.11% respectively and vanadium recoveries have been of the order of 90%, 60% and 86% respectively. Thus, as a vanadium additive, the performance of VO_xCy is well comparable to that of Fe-V. Employing the same oxy-carbide as a soluble anode, it has also been possible to prepare the metal at a cathode current efficiency of 92% by fused salt electrolysis at 900°C and c.c.d. of 325 A/ft² in a halide bath containing 4 wt% of soluble vanadium.

1.9.2 Preparation of Hf-Ta alloy by Carbide-Oxide Reduction
(HfC and Ta₂O₅)
(S.P. Garg, R. Venkataramani and C.V. Sundaram)

Hf-Ta alloys possess good high temperature and creep resistance properties and find application in aero-space industries. The alloy containing about 48-53% Ta has been successfully produced by interacting HfC with Ta₂O₅ at 2000°C under a vacuum of 10⁻⁴ torr.

Pellets made from a mixture of HfC and Ta₂O₅ are progressively heated to a temperature of 2000°C under a dynamic vacuum of 10⁻² to 10⁻⁴ torr in a vacuum induction furnace. Almost 70% of the reduction takes place during the heating process. Hf-Ta alloys are obtained in the form of a button by melting the pre-reduced pellets for 2 hrs. in an electron beam furnace. The alloy analyzing about 50% Ta indicated a button hardness of 560 VHN which is comparable to the hardness of the alloy obtained by direct melting of Hf and Ta. Alloys with low oxygen and carbon contents (30 ppm and 0.29% respectively) have been produced by this method. The

influence of the oxygen to carbon ratio (O/C) in the charge on the extent of pre-reduction and final purity of the alloy has been examined in detail and the results are given in Table-II.

TABLE II
INFLUENCE OF OXYGEN/CARBON RATIO ON THE
PURITY OF CARBIDE-OXIDE REDUCED Hf-Ta
ALLOYS

Charge Composition	Reduction Achieved		Analysis of Hf-Ta Alloys			Hardness (VPN)
	during Heat Soaking at		after Electron Beam Melting			
O/C Ratio	1650°C	2000°C	wt %			
	x 10 ⁻⁴ torr	x 10 ⁻⁴ torr	Ta	C	O	
0.95	28.8	67.5	47.9	0.88	0.040	538
1.00	28.3	71.7	47.8	0.61	0.009	498
1.05	30.6	68.4	50.7	0.39	0.003	488
1.10	31.6	69.0	52.6	0.36	0.018	505
1.15	32.5	63.2	53.3	0.29	0.029	577

1.10 ULTRAPURIFICATION

1.10.1 Iodide Refining of Reactive Metals

(V.D. Shah, B.P. Sharma and C.M. Paul)

Work on the preparation of high purity Zr, Ti and Hf by the iodide process has been continued during the year mainly to meet the requirements of these metals from within the Division.

In the growing of crystal bar Ti the influence of crude metal temperature on the deposition rate of pure metal was studied in detail and the results are given in Table-III.

TABLE III
INFLUENCE OF CRUDE METAL TEMPERATURE ON
THE GROWING OF CRYSTAL BAR TITANIUM

Crude Metal Temperature °C	Growth Rate	
	gms/hr/cm length	mbos/hr/cm length
100	0.0086 (initial rate which gradually decreased to zero after a few hours)	0.439
150	0.0160 (initial rate which gradually decreased to zero after a few hours)	0.0110
600	0.0130	0.006
650	0.0250	0.011
700	0.0700	0.031
750	0.0960	0.0426
800	0.0932	0.0406

In the starting of the experiment with a filament temperature of 1300°C and a crude metal temperature of 150-200°C, a very low growth

rate has been observed which gradually decreased and virtually stopped after a couple of hours. Even on starting a fresh experiment at a lower crude metal temperature (100-150°C), the same phenomenon has been observed. On increasing the crude metal temperature in steps of 100°C and keeping the filament temperature steady at 1300°C, no noticeable growth rate was observed upto 600°C. However the growth again started at 600-650°C and has become appreciable above 700°C. With the filament temperature maintained at 1300°C the growth rate has come to a maximum of about 0.1 gm/hr/cm-length when the feed metal temperature has been 750°C. By increasing the feed metal temperature to 800°C, there has been no appreciable variation in the growth rate. The eventual stoppage of growth at the low crude metal temperatures is attributed to the conversion of TiI_4 to the less volatile TiI_2 by reaction with the feed material present in excess of the stoichiometric requirement. However by increasing the feed metal temperature, it has become possible to elevate the vapour pressure of TiI_2 and achieve appreciable growth.

Detailed investigations have also been carried out on the preparation of crystal bar hafnium starting from hafnium metal pellets obtained by compaction and sintering of Hf-powder produced by the Ca-reduction of HfO_2 . A maximum growth rate of about 0.1 gms/hr/cm-length has been observed for a sponge temperature of 325°C and filament temperature of 1400°C. Substantial purification of the crude Hf metal has been possible by iodide refining with respect to all non metallic and most of the metallic impurities. The distribution of various impurities in the crude metal and in the crystal bar is given in Table-IV.

TABLE IV

ANALYSIS OF FEED MATERIAL AND CRYSTAL BAR
HAFNIUM

(All values are in ppm unless otherwise specified)

Impurities	Feed material - Sintered pellets of Ca-reduced hafnium powder	Crystal bar hafnium
Fe	580	110
Cr	30	10
Mg	13	13
Zr	13.0 %	19.4 %
N	250	22
O	6900	172
H	-	5
C	-	44

1.10.2 Ultrapurification by Electron Beam Floating
Zone Refining

(B.P. Sharma, V.D. Shah and C.M. Paul)

The 1.25 KW electron beam floating zone refining unit designed earlier has been fabricated, assembled and commissioned. The refining chamber is a 150 mm dia x 750 mm long glass tube in which the electron beam heating filament is held stationary and the molten zone is made to travel by moving the specimen rod with the help of a constant speed electric motor coupled to a gear system. The capability of the unit for refining 6 mm dia zirconium rod has been successfully tested. It has

been found that although the unit is capable of melting the specimen rod and producing the molten zone, the driving mechanism for moving the specimen needs modification. The driving mechanism is presently being modified to provide slow, smooth and continuous motion to the specimen rod during refinement.

1.11 OTHER PROGRAMMES

1.11.1 Determination of Sintering Characteristics of UO_2 Powders by DTA and TGA Technique (S.P. Garg and R. Venkataramani)

A knowledge of the sintering characteristics of UO_2 powders is very important in controlling the properties of sintered compacts. In view of this, investigations have been carried out to determine (i) temperature of oxidation of UO_2 powders to U_3O_7 by TGA technique, and (ii) amount of heat released during annealing of these powders at temperatures upto $1500^\circ C$ in inert atmospheres. Both the temperature of oxidation and the heat released are related to strain energy and surface activity of the powder.

UO_2 powders having different sinterabilities have been prepared by heat soaking UO_2 powder (obtained from ammonium diuranate) at $1000^\circ C$ and $1300^\circ C$ for different periods of time (1 to 10 hours) in hydrogen atmosphere.

The temperatures of oxidation of each of these annealed powders has been determined by TGA technique in Mettler Thermoanalyser and the results are given in Table-V.

TABLE V
TEMPERATURE OF OXIDATION OF UO_2 to
 U_3O_8

UO ₂ Powder Sintered in Hydrogen		Temperature of Oxidation	Rate of Oxidation	Weight Gain for U ₃ O ₈ Formation
Temp °C	Soaking Period hours	°C	mg/min	mg/gm
1000°C	1	188	0.57	36.00
	5	192	0.43	37.75
	10	196	0.44	38.00
1300°C	1	200	0.51	38.00
	5	240	0.39	37.50

Temperature of oxidation of UO_2 powder not sintered in H_2 has been found to be 178°C. As can be seen from the table, temperature of oxidation (UO_2 to U_3O_8) steadily increases with sintering temperature and time of heat soak in H_2 atmosphere.

1.11.2 Thermodynamics of Ti-O-C System
(S.P. Garg, J.M. Juneja and Y.J. Bhatt)

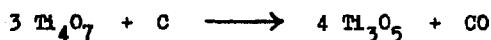
Carbothermic reduction of an oxide is an established route for the preparation of refractory metals and their carbides. Thermodynamic studies of these oxide-carbon and oxide-carbide systems are thus of relevance in the process metallurgy of refractory metals and their carbides.

Investigations have been carried out to study the thermodynamics of Ti-C-O system. The study involves measurement of equilibrium pressures of CO over mixtures of oxides like Ti_3O_5 - Ti_4O_7 and Ti_2O_3 - Ti_3O_5 and carbon (employing Hg-manometer) in the temperature range 1160-1350°K. The oxide mixtures have been prepared by argon arc melting of a charge consisting of TiO_2 and Ti-metal powder. The presence of various phases has been confirmed by X-ray analysis.

The equilibrium P_{CO} values have been measured as a function of temperature for the above mixture of oxides and carbon. The equilibrium pressure (p_{CO}) data could be represented by

$$\log P_{CO} = -\frac{A}{T} + B$$

From the above equation ΔF_R° was calculated for the reactions



Knowing the value of the free energy of formation of CO, the free energies of formation of Ti_3O_5 and Ti_4O_7 have been calculated and found to be in good agreement with the values reported earlier by Vasileva* and Kubaschewski**. The thermodynamic data of the reactions are given in the table below

TABLE VI
THERMODYNAMIC DATA ON REACTIONS OF
OXIDES OF TITANIUM

Reaction	ΔF_{1200K}°		ΔH°		ΔS°	
	Present work	Reported value	Present work	Reported value	Present work	Reported value
	Kcal	Kcal	Kcal	Kcal	cal/deg	Cal/deg
$8 \text{Ti}_3\text{O}_5 + \text{O}_2$ $= 6 \text{Ti}_4\text{O}_7$	116.88	116.66*	118.56	168.88*	1.40	42.6*
$6 \text{Ti}_2\text{O}_3 + \text{O}_2$ $= 4 \text{Ti}_3\text{O}_5$	125.14	129.72**	158.72	177.0**	27.98	39.4**

1.11.3 Thermodynamics of Al-Mg System by Vapour Pressure Measurement
(S.F. Garg and Y.J. Bhatt)

Thermodynamic properties of liquid Al-Mg alloys have been studied by measuring the vapour-pressure of Mg over liquid Al-Mg alloys (5 to 94 atom % Mg) at various temperatures in the range of 900-1245°K by employing transpiration technique. From the experimentally obtained vapour pressure data various thermodynamic properties of the alloys have been calculated and compared with the values already reported. Attempts have also been made to calculate the Mg activity by solubility measurement of Mg in MgCl_2 while equilibrating with Al-Mg alloys, and also by phase diagram studies of Al-Mg system. It has been found that the activity of Mg in liquid Al-Mg system nearly conforms to the ideal solution behaviour at 1000 K with only slight negative deviation in the Mg rich region.

1.11.4 Thermodynamic Investigations Using Solid State EMF Measurements

(S.P. Garg and J.M. Juneja)

Work has been initiated to make EMF measurements of the following solid state cell :



The CaF_2 solid electrolyte separates the two electrode compartments. After assembling the cell it has been evacuated and flushed with purified argon gas. The cell is then heated slowly in an atmosphere of flowing purified argon gas (flow rate 50 cc/min). The EMF of the cell has been measured at various temperatures and the EMF values plotted against temperature. The straight line relationship obtained for the above cell has been represented by the equation

$$E(\text{volt}) = 0.0245 + 0.120 \times 10^{-3} T$$

The cell reaction taking place can be represented by the equation



The standard free energy change ΔF for this reaction has been calculated using the relation

$$\Delta F = -nFE$$

(where $n = 2$ for the above reaction and $F = 23062$ cal/volt) and can be represented as

$$\Delta F(\text{cal}) = -1130 - 5.535 T$$

The results are in close agreement with the values reported in the literature.

2. PHYSICAL METALLURGY

The Physical Metallurgy Section has been mainly concerned with the study of the physical and mechanical properties of metals and alloys of interest to the nuclear energy programme.

Three groups - Mechanical Metallurgy, Structural Metallurgy and Metal Physics - have been actively engaged in investigations covering a wide range of properties of Zr-base alloys, and on R & D work on a number of problems of nuclear interest.

The Mechanical Metallurgy Group has been investigating the grain size effect, alloy hardening, stress relaxation and thermally activated deformation processes. Fracture studies on end shield materials, and also elastic and anelastic behaviour of Zr alloys have also been conducted.

The Structural Metallurgy Group has been carrying out transmission electron microscopic studies on phase transformations on Zr and Ti and their alloys and on stainless steels. Extensive work has earlier been carried out on martensitic transformations in Zr and Ti-base alloys and during the current year emphasis has been shifted to eutectoid transformations and precipitation reactions. Scanning electron microscopic investigations have been carried out on several service failures and for powder metallurgy work.

The Metal Physics Group has been continuing its studies on diffusion phenomena and impurities in bcc transition metals and interdiffusion studies in isomorphous systems. It is utilising the Electron Microprobe Analyser for diffusion studies as well as for the study of growth kinetics and intermetallic phases on various alloys. Nucleation and growth of gas bubbles in irradiated copper-boron alloys and solidification structure in alloys have also been carried out. The work carried out on neutron irradiated nickel alloys and irradiation hardening in Zr and Zr-base alloys has also been reported during the current year.

The acquisition of latest models of transmission and scanning electron microscopes and their successful commissioning during this year has greatly facilitated several investigations carried out by the Division.

Physical Metallurgy Section continues to give valuable assistance in various metallurgical problems referred to it by other Divisions of B.A.R.C. and outside agencies as well.

2.1 MECHANICAL METALLURGY

2.1.1 Internal Stress Variation in Zircaloy-2 (P. Dasgupta)

In the thermal activation analysis of a deformation process, internal stress developed in a material is assumed to be independent of temperature. Work was carried out to confirm whether this is valid for Zircaloy-2. Accordingly, a stress relaxation technique has been adopted where the stress was relaxed for sufficiently long time till it approached σ_{μ} and then the temperature of the specimen was changed quickly. It has been observed that even after sufficient time for load relaxation, the relaxed load does not reach the initial value suggesting that variation of σ_{μ} with temperature is a real one. From this it could be inferred that the structure, arrangement and distribution of dislocations which contribute to internal stress are a function of temperature. Further support for the above findings has been obtained from the work-hardening studies on Zircaloy-2, where work hardening rate was found to depend on temperature.

2.1.2 Stress Relaxation and Dislocation Densities in Zirconium and its Alloys (P. Dasgupta)

Room temperature stress relaxation experiments have been conducted with Zr-oxygen, Zircaloy-2 and Zr-Ti alloys in order to ascertain the constancy of mobile dislocation densities during the stress relaxation process. It has been observed that the master

relaxation curve and stress relaxation from the initial stress level did not superimpose suggesting that the assumption of constancy of structure during stress relaxation is not strictly valid. The differences in the magnitude of the relaxation rate between the two curves were found to be more pronounced with increase in total plastic strain. Dynamic recovery is suggested to be the dominant mechanism causing structural changes during the stress relaxation process with consequent alteration in mobile dislocation densities.

2.1.3 Computer Technique for Determination of Strain Rates (V. Raman and P. Dasgupta)

A computer simulation programme for accurate computation of strain rate parameter during stress relaxation has been initiated. The programme involves either graphical differentiation of the curve using a set of points close to predetermined points or formulating a polynomial, which defined the experimental curve as closely as possible and solving the polynomial using appropriate data points. Both the methods were tried for Zircaloy-2 and the technique of graphical differentiation was found to be more appropriate. Application of this programme to various other metals and alloys is being attempted.

2.1.4 Fracture Studies of Zr-1at%Ti with Various Oxygen Levels (V. Raman, S. Mishra and P. Dasgupta)

Oxygen plays a vital role in influencing the fracture modes of zirconium and its alloys. Accordingly fracture studies were conducted with an alloy of Zr-1at%Ti containing various levels of oxygen. Oxygen was introduced in specimens by soaking the samples at 800°C under oxygen pressures of 3, 6, 9, 12, 15, 18 and 21 mm of Hg for 7 days. Hardness measurements on samples exhibited a progressive increase in VHN values indicating that oxygen concentrations are higher for specimens exposed to higher gas pressures. Examination of the fracture surface of the specimens under SEM showed gradual change in the mode of fracture from ductile to almost brittle behaviour.

Ductile fractures were associated with large slip traces introduced by occurrence of both primary and secondary slip with concomitant recovery process. This implies that shear mechanism played a dominant role in nucleating the crack embryo which latter propagated due to deformation-induced stresses in the material. Fractography of high oxygen alloys exhibited strain induced twin traces. River patterns on fracture surface were also observed under high magnification.

2.1.5 Anomalous Stress-Strain Behaviour of Pure Polycrystalline Zirconium
(P. Dasgupta)

Examination of the stress-strain behaviour of iodide zirconium under compression exhibited various stages. This is analogous to single crystal deformation curve where each stage has its characteristic features. Metallographic examination of the compressed sample at various strain levels indicates gradual change over from single slip mode to multiple slip operation during stage II. The incidence of cross slip has also been observed at Stage III. The real cause of this unfamiliar polycrystal deformation behaviour under compression is yet to be explored quantitatively.

2.1.6 Thermomechanical Treatment of Zr-2.5Nb - 0.5Cu Alloy
(V. Raman, T.K. Sinha and P. Dasgupta)

Zr-2.5Nb-0.5Cu alloy is used as calandria pressure tube spacers (in the form of garter springs) in CANDU type reactors. A programme has been initiated to make detailed systematic heat treatment studies coupled with useful mechanical properties evaluation on this material. Accordingly, the prepared material of this composition was quenched from beta region (900°C) and aged at 540°C for 2, 4, 6, 8, 24 and 60 hours. Hardness measurement showed progressive increase in VHN values with no incubation period. Rate of increase in hardness in the initial stage was found to be more rapid than in long time ageing. Examination of microstructure of the

samples revealed that quenched specimens developed martensitic structure while the aged one revealed the presence of fine second phase precipitates. The volume fraction of the precipitates increases with ageing time. Mechanical properties evaluation is under progress.

2.1.7 Strain Rate Sensitivity of Cold-worked Zircaloy-2 (T.K. Sinha)

The analysis of the service performance of engineering materials under stressed condition requires a precise knowledge of their strain rate sensitivity parameter (m^*) expressed by the following relation $\partial \ln \dot{\epsilon} / \partial \ln \sigma$ or $d\sigma/d \ln \dot{\epsilon}$. Since Zircaloy-2 is used in the cold worked stage it is essential to have a precise knowledge of its strain rate sensitivity at reactor operating temperature. As a first step, attempts were made to find out m^* at room temperature using strain rate cycling method. Because of poor ductility of the material this method gave m^* with wide variations. To overcome this difficulty, a stress relaxation technique has been adopted and estimation of m^* parameter is in progress.

2.1.8 Mechanical Behaviour of Heat-Treated Binary Zr Alloys (V. Raman and P. Dasgupta)

As part of the Zr-alloy development programme with emphasis on developing suitable alloys with improved mechanical properties, a series of Zr alloys having the composition Zr-1.5 Sn, Zr-2.5 Cu, Zr-1.6 Cu, Zr-1 Cr, Zr-4 Al, Zr-7 Al, Zr-10 Al have been chosen. These alloy compositions have been prepared by non-consumable arc melting. Fabrication of Zr-1.5 Sn, Zr-2.5 Cu, Zr-1.6 Cu, Zr-1Cr in the form of sheets by hot rolling (after prior encapsulation in vacuum) has also been completed. The conventional technique of hot rolling could not be applied to Zr-Al alloys because of their inherent brittleness, and a modified technique is being tried to obtain mechanical testing specimens. A systematic

investigation on the mechanical behaviour of heat treated Zr-1.5 Sn alloy has been completed. The heat treatment programme involved water quenching the samples from 830°C, 900°C and 1000°C after one hour soaking at respective temperatures, and the water quenched samples were aged at 550°C for 4 hours. The work hardening behaviour of this material has been analysed on the basis of two equations $\sigma = K \epsilon^n$ and $\sigma = \sigma_0 + h \epsilon_p^m$. The plot of log work hardening rate as a function of true plastic strain for water quenched samples exhibited single stage and the work ^{hardening} rates were found to decrease monotonically with increase of plastic strain. In the case of aged samples, two distinct stages were observed, the onset of stage II depending on the quenching temperature. Higher quenching temperature favours the earlier initiation of Stage II at low plastic strain values. The log σ as a function of log ϵ_p also showed similar trend. Heat-treatment and mechanical property studies with other alloys are in progress.

2.1.9 Radiation Embrittlement Studies on End Shields for RAPP and MAPP
(P. Dasgupta)

Impact property evaluation of end shield material in the unirradiated condition has been carried out with specimen geometry following Charpy V-notch substandard size. Energy absorbed values vary from 1 ftlb to 82 ftlb in the temperature range of 77 to 373°K. The first batch of 32 samples irradiated at a fluence level of 1.5×10^9 n/cm² has been taken out from CIRUS and is at present undergoing cooling before being tested for impact property determination. Another batch of 32 samples has been loaded to receive a fluence level of 3×10^{19} n/cm². Specimen design and the formulation of test proposal for fracture mechanics studies are in progress.

2.1.10 Dynamic Strain Ageing Behaviour of Zircaloy-2
(V. Raman and P. Dasgupta)

Presence of interstitials in zirconium alloys may cause

strain ageing that can result in loss in ductility, thereby restricting the service application of these alloys. To examine this problem, an attempt has been made to study the dynamic strain ageing behaviour of zircaloy-2. Annealed samples of zircaloy-2 having a grain size 15-20 μ have been tested at temperatures between 250°C and 350°C, at strain rates of $1.6 \times 10^{-3} \text{ sec}^{-1}$ and $3.2 \times 10^{-3} \text{ sec}^{-1}$. No detectable serrations in the stress-strain curve have been observed which indicates that temperature and strain rate ranges are not appropriate to cause solute-dislocation interaction effective enough for dynamic strain ageing. Temperatures above 350°C and strain rates less than 10^{-3} sec^{-1} could be a better choice for observing this effect in Zircaloy-2.

2.1.11 Alloy Development Programme

(M.K. Asurdi, T.K. Sirha, P. Dasgupta and V. Raman)

Sufficient progress has been made towards standardisation of melting, fabrication and heat treatment procedures of Zr-2.5Nb alloy which has been proposed as a pressure tube material in nuclear power reactors. Melting parameters involved in consumable electrode melting of sponge as well as Zr-2.5 Nb alloy were determined, and on this basis, an ingot of Zr-2.5 Nb having the dimension of 44 mm dia. and 150 mm. length was melted using pressed Zr-sponge and Nb-wire electrode. Metallographic examination of the first melted ingot showed segregation of alloying element at the central region and therefore remelting was necessary to obtain a homogeneous ingot.

The quality of the double arc melted alloy has been evaluated by metallography and hardness measurement. The hardness value has been found to be within 210-220 VHN which compares favourably with the reported hardness for commercial Zr-2.5 Nb alloy - in the cast form. Metallographic examination of the samples sectioned at different regions of the ingot showed a uniform microstructure consisting of primary Nb-rich beta-dendrites embedded in the matrix of transformed beta. Sections hot rolled at $\approx 850^\circ\text{C}$, when examined, showed fine recrystallised alpha together with a fine network of transformed beta.

phases. The rolled sheet, when solution annealed at 850° (alpha + beta region) and water quenched, developed a microstructure consisting of primary alpha embedded in alpha' martensite. The hardness of the quenched sample was found to increase to 270-280 VHN.

To sum up, metallographic examination and hardness measurements carried out on cast, rolled and heat-treated samples of Zr-2.5 Nb prepared in this laboratory have shown characteristics closely similar to those reported for commercial grade Zr-2.5 Nb alloy. Further work on heat-treatment and mechanical properties is continuing.

2.1.12 Internal Friction Studies in Stable and Metastable Beta Titanium Alloys

(S. Mishra and M.K. Asundi)

Internal friction studies were conducted on Ti-Mo and Ti-V binary alloys, and a beta III alloy (Ti-11.5 Mo-6 Zr-4.5Sn - 0.13 O). Five peaks were observed out of which only one has been reported earlier. The peak which occurs at the lowest temperature has been reinterpreted as due to the jumping of vacancies around interstitials leading to rotation of vacancy-interstitial solute pairs. The fourth peak is interpreted as due to Snoek relaxation. The fifth peak is interpreted as due to dislocations generated during isothermal ω transformation. The binding energy of oxygen with dislocation is the difference between the activation energies of the last two peaks and it has been found to be 5 kcal/mole. Another peak has been observed in Ti-17%Mo alloy containing low oxygen. This has been explained as due to the athermal formation and dissolution of the embryos of ω under cyclic stress.

2.1.13 Discontinuous Yielding in Solid Solutions

(V.V. Raman, C.N. Rao and M.K. Asundi)

Many solid solutions at certain ranges of temperature and strain rate exhibit discontinuity in the stress strain curve. Such alloys also exhibit a decrease in flow stress for an increase in strain rate with a range of temperature. A model capable of explaining

this phenomenon has been formulated. The model assumes the following:

- (1) At any given time only a fraction of the dislocations are mobile
- (2) All dislocations are mobile for sometime and stationary for the rest of the time
- (3) When the dislocations are stationary, solute atmospheres start forming around them and when they are in motion, they move dragging the atmospheres which gradually decay and release the dislocations. The metallurgical behaviour of the material would correspond to the observed negative strain rate sensitivity and hence to discontinuous yielding.

2.1.14 Thermomechanical Treatment in Zircaloy

(V.V. Raman, C.H. Rao and M.K. Asundi)

Texture and grain size are the two important variables that can be controlled to give desired mechanical properties to zircaloy-2. The texture of zircaloy-2 sheets is affected by the variables during hot rolling and cold rolling operations. It is also affected by intermediate annealing schedules during cold rolling operation. Grain size, on the other hand, depends on the last stages of cold rolling operation and annealing time and temperature. Different combinations of the above variables were used with the same starting material to end up with a sheet of the same thickness. The yield strength, ultimate tensile strength and elongation were studied as a function of these variables.

2.1.15 Oxygen Dislocation Binding in the Beta Titanium Alloys

(S. Mishra and M.K. Asundi)

One of the ways to determine the binding energy of solutes to dislocations is from their enhanced concentration around the dislocation. The concentration of solutes along the dislocation, on the other hand, can be measured by studying the amplitude dependence of internal friction. Granato and Lucke have shown that the amplitude dependent internal friction due to breakaway of dislocations from solute atoms would follow a relation $C_1/\xi \exp(-C_2/\xi)$ where C_1 and C_2 are constants and ξ the strain amplitude. The constant C_2

is proportional to the concentration of solute atoms along the dislocations. Hence from C_2 values at different temperatures one can calculate the binding energy of the solutes with the dislocations. Such studies were carried out in Ti-45%Mo and Ti-56%V alloys between 375°C and 550°C. It was found that the binding energy of oxygen with dislocation in Ti-56V alloy is three times as much as that in Ti-45 Mo alloy. This is consistent with the expectation since the radii of the octahedral holes in the two alloys are different, giving rise to different elastic interaction energies.

2.1.16 Effect of Fatigue Hardening on Annealing Characteristics in Zirconium Alloys (V.V. Raman)

Fatigue hardening in metals and alloys is a well known phenomenon. Under cyclic stresses, well below the yield strength, substructural changes take place in metals which result in substantial changes in their properties after many such cycles. In polycrystalline zirconium alloys, macroscopic flow is possible only if some twin systems also start operating. However, during cycling between two stresses, localized dislocation multiplication by stress concentration around crack tips of fatigue induced cracks can cause localized hardening and also vary the annealing characteristics. This is being investigated.

2.2 STRUCTURAL METALLURGY

2.2.1 Phase Transformation in Zirconium Alloys

(1) Eutectoid Decomposition in Zr-Cu Alloys

(P. Mukhopadhyay, S. Banerjee and R. Krishnan)

Eutectoid decomposition in some zirconium alloys has been reported to be very rapid and such alloy systems are designated as "active eutectoid" systems. An attempt has been made here to study the mechanism of the active eutectoid decomposition process in Zr-Cu alloys. In a Zr-1.6%Cu alloy (eutectoid composition), water quenching

from the beta phase has been found to produce a structure consisting of several colonies, each containing either an aggregate of two twin related alpha orientations interspersed with one another or a mixture of an alpha orientation and a metastable second phase orientation arranged in a lamellar fashion. In many regions, the 'wavy' second phase lamellae have been observed to emerge from the straight twin lamellae. Though the majority of the colonies are of irregular shape, characteristic of the product of a cellular reaction, in some regions, planar boundaries, typical of a martensite habit have been observed. An order of magnitude estimate of the growth rate of a colony has been carried out using parameters like the observed interlamellar spacing and the reported values of diffusion coefficients. It has been found that the observed growth rate is a few orders of magnitude faster than the estimated rate. Taking all these points into consideration, it has been suggested that the reaction involves the simultaneous operation of a martensitic and a cellular reaction.

Studies on a hypoeutectoid alloy (Zr-0.75%Cu) have also indicated a shear transformation leading to the formation of martensite laths and a simultaneous eutectoid reaction producing a lamellar distribution of a metastable second phase at the lath boundaries, during the beta-quenching treatment. Thermodynamically a reaction of this kind is feasible because the supercooling required for initiating the martensitic transformation is adequate to bring this hypoeutectoid alloy into the region of direct eutectoid transformation.

(ii) Evolution of Different Microstructures in Zr_3Al Base Alloys
(P. Mukhopadhyay, V. Raman, S. Banerjee and R. Krishnan)

Zr_3Al base alloys have shown some promise as structural materials in nuclear power reactors. This intermetallic compound has adequate formability at elevated temperatures ($> 1050^\circ C$) and unlike alpha Zr-Al alloys, it has a good corrosion resistance. Both hypo and hyper stoichiometric compositions were chosen for this study.

In the hypostoichiometric alloy (Zr-4.2%Al), beta quenching produced a lath martensite, a structure which was found to contain micro domains of ordered hexagonal DO_{19} particles in a matrix of disordered alpha. During tempering at temperatures $\geq 800^\circ\text{C}$, the Zr_3Al phase was found to emerge in a lamellar form from the lath boundaries. The transformation front was seen to advance in a discontinuous manner, finally producing a lamellar distribution of the alpha phase and the Zr_3Al phase (LL_2 structure) with the following orientation relation :

$$\{0001\}_{DO_{19}} \parallel \{111\}_{LL_2}$$

In the hyperstoichiometric alloy (Zr-10%Al), quenching from the $\beta + Zr_2Al$ phase field produced a structure consisting of the Zr_2Al phase dispersed in a transformed beta matrix. During ageing at 800°C , the alpha phase was found to react with Zr_2Al to form a mixture of alpha and Zr_3Al phases.

(iii) Precipitation in Zirconium-tin Alloys:

(Smt. Uma Naik and S. Banerjee)

In standardizing the fabrication schedule of zircaloy-2, considerable difficulty has been experienced in dissolving the second phase. The exact nature of this second phase has not been identified yet. In view of this, the present work was carried out on a binary Zr-1.5% Sn alloy. Transmission electron microscopy was used to detect the fine precipitates which form in this alloy during the quenching from the β , the $\alpha + \beta$ and the α phase fields. Selected area diffraction and dark field techniques were employed to identify the structure of the precipitating phase. The coherency strain associated with these precipitates was seen to produce a strong contrast. This contrast is being analysed in order to be able to determine the magnitudes of this strain in different directions. During ageing at 550°C , the precipitates were seen to grow at a very slow rate.

2.2.2 Shape Memory Effect

(S. Banerjee and V.V. Raman)

Some martensitic materials have been reported to have a 'memory' of their original shape, however, arbitrary. If this shape is distorted by a plastic deformation and subsequently the material is subjected to an appropriate thermal cycle, the original shape of the material is regained. This phenomenon has been attributed to the deformation process due to the irreversible migration of coherent interfaces resulting in a change either in the structure or in the orientation distribution of the crystals constituting the material. In the present investigation, a set of experiments has been carried out where Ni-50 at% Ti alloy martensite samples have been subjected to a strain and thermal cycle while continuously recording the stress generated in these samples. The results of these experiments have provided information regarding the spring back action. The effect of variables like the plastic strain level and the residual stress level at which the thermal cycle is given, the temperatures and the duration of the thermal cycle etc. on the stress generated during the shape recovery process has been examined. Electron microscopic investigation has shown that Ni-Ti martensite plates, made up of an alternate stacking of two twin related orientations, also contain some blocks of twin orientations within the matrix lamellae. This observation is indicative of the ease with which reorientation is possible in this structure.

2.2.3 Heat Treatment of Titanium and Zirconium Alloys

(1) Ti-8Al-1Mo-1V

(S.J. Vijayakar, S. Banerjee and R. Krishnan)

A wide variety of microstructures could be produced in this commercial alloy by choosing suitable heat-treatments. In this study, the microstructures were characterized from TEM observations and the mechanical properties corresponding to these structures

were evaluated. By changing the solutionizing temperature in the $(\alpha + \beta)$ phase field, the relative proportions and compositions of the alpha and the beta phases could be altered. On quenching from these temperatures, the beta phase was found either to transform into a martensite or be retained, depending on the re-distribution of the alpha stabilizing (Al) and the beta stabilizing (Mo & V) elements in the beta phase during the solutionizing treatment. The plot of the yield strength versus the solutionizing temperature showed a minimum which was found to be associated with the presence of the metastable beta phase. During deformation, this beta phase was found to undergo a martensitic transformation, the 'yield stress' representing the critical stress required for inducing the transformation. Such yielding at that relatively low stress level did not occur when the solution treated material was subsequently tempered in order to decompose the metastable beta phase into an equilibrium mixture of alpha and beta. In some cases, where the solutionizing temperature was brought down to $\leq 900^\circ\text{C}$, the alpha phase got enriched in aluminium to about 10% resulting in the formation of the ordered α_2 phase.

(ii) Ti-6%Cr and Ti-12%Mo

(M. Unnikrishnan and S. Banerjee)

The precipitation of the alpha phase in the matrix during isothermal treatments of these two alloys was studied. The kinetics of these precipitation reactions were examined, the C-shaped time-temperature-transformation diagrams were plotted and the activation energy of the process evaluated. In the Ti-6%Cr alloy, it was seen that the reaction rate for samples quenched from the beta phase and subsequently tempered in the $(\alpha + \beta)$ phase field was much higher than that for the samples directly quenched from the beta phase to the reaction temperature in the $(\alpha + \beta)$ phase field. TEM investigations showed that even a single precipitated alpha plate was constituted of a number of alpha crystals of differing orientations. In many cases the matrix beta was found to undergo a martensitic reaction.

(iii) Mechanical Properties of Quenched and Tempered Zr-Nb Alloys
(S.J. Vijayakar and S. Banerjee)

In continuation of the previous work on the structural investigation of quenched and tempered Zr-Nb alloys, a study of the mechanical properties of the heat treated Zr-2.5%Nb and Zr-5.5%Nb alloys was taken up. By selecting the proper tempering temperatures, it was possible to precipitate the β_1 phase (Zr-20%Nb) in one set of samples and the β_2 phase (Nb-15%Zr) in another set. From the results obtained so far, it has been possible to infer that the maximum strength is associated with the precipitation of the β_1 phase at temperatures slightly lower than the monotectoid temperature. When the tempering temperature is raised above the monotectoid temperature a rapid coarsening of the β_1 precipitates occurs, leading to a conspicuous drop in the strength of the alloy.

2.2.4 Studies on Transformation in Steels

(1) Deformation-induced Transformations in a Type 316 Stainless Steel (V. Seetharaman, S. Banerjee and R. Krishnan)

In many austenitic steels, austenite transforms to martensite during plastic deformation at or below ambient temperature. Such a deformation induced transformation manifests itself as the well known TRIP effect in these steels and has a pronounced influence on several characteristics like the resistance to crack propagation, magnetic permeability, corrosion resistance etc. Therefore, experiments have been carried out to study the formation of martensite as a function of the temperature, the rate and the extent of deformation and its effect on the mechanical properties of this steel. It has been found that plastic deformation at temperatures below -70°C results in the formation of thin and narrow deformation bands on $\{111\}$ and these bands, in general consist of overlapping stacking faults, mechanical twins and sheets of hexagonal close packed ϵ phase. Upon further deformation, the ϵ phase nucleates at the intersection

of two sets of shear bands and then grows into a lath like morphology. Once α is nucleated by deformation at sub-zero temperatures, it could then grow spontaneously during subsequent heating. This thermally activated growth of α is rapid around 400°C, but above 500°C, α reverts back to austenite. The formation of α martensite leads to pronounced strengthening of this steel and the increments in the flow stress values could be directly correlated with the volume fraction of the α phase.

(ii) Precipitation Reactions at Elevated Temperatures in a Type 316 Stainless Steel

(V. Seetharaman)

Long time exposure of type 316 stainless steel to elevated temperatures is known to cause decomposition of the austenitic matrix resulting in the formation of several carbides and inter-metallic phases. Unfortunately, the time and temperature ranges reported by different investigators for the formation and stability of the various phases are not consistent. Hence a systematic investigation of the microstructural stability of this steel as a function of thermal and mechanical pretreatments has been taken up. In the case of solution treated alloys, ageing treatments lasting upto 250 hours ^{and} temperatures ranging from 600°C to 800°C cause only the precipitation of carbide and the χ phase. Initially, $M_{23}C_6$ type of carbides precipitate profusely along the grain boundaries and twin boundaries. But after prolonged ageing a large number of intragranular Widmanstätten precipitates also appear. $M_{23}C_6$ type carbides possess a f.c.c. structure and are in parallel orientation with the matrix.

Cold working prior to ageing enhances the precipitation kinetics and renders the distribution of precipitates more uniform. The deformation bands present in the cold worked austenite act as preferential nucleation sites for these carbides. Since the overall volume fractions of the precipitates remain below 1% even after very long durations of ageing, these precipitates do not contribute significantly towards the strengthening of this steel. However,

they give rise to a strong tendency for the cracks to propagate along the grain boundaries containing these precipitates.

(iii) Age Hardening in a PH 13-8 Mo Stainless Steel
(V. Seetharaman and M. Sundara Raman)

Martensitic precipitation-hardenable stainless steels are noted for their high fracture toughness, resistance to stress corrosion cracking and retention of high strength at temperatures as high as 500°C. Among them PH 13-8 Mo stainless steel is characterized by the complete absence of δ -ferrite and hence possesses good centerline transverse ductility. This work has been taken up to follow the microstructural changes occurring during the precipitation hardening treatment and to study their effects on the mechanical properties of this steel.

Solution treatment at 900°C followed by air cooling leads to the complete transformation of austenite to martensite. This martensite consists of very fine laths and is characterized by a high density of dislocations. Subsequent ageing of this martensite at temperatures ranging from 450°C to 600°C leads to the formation of extremely fine precipitates of an intermetallic compound corresponding to the composition, NiAl. Besides, a fine scale precipitation of reverted austenite has been observed in samples aged at 525°C and these austenite precipitates coarsen rapidly during ageing at higher temperatures.

It has been found that ageing at any temperature between 460°C and 575°C results in a substantial strengthening of this steel. The yield strength and ultimate tensile strength values reach a maximum after ageing at 525°C. This increase in strength is not accompanied by any significant reduction in ductility. Stress relaxation experiments show that the increase in flow stress values after ageing is mainly due to the increase in the athermal component of flow stress. It appears that the strengthening due to NiAl precipitates arises mainly from the internal stresses in the matrix, while that due to the austenite precipitates is the result of the relative misorientation of the slip systems in the matrix and the precipitates.

2.3 METAL PHYSICS

2.3.1 Diffusion Studies

(1) Self Diffusion in Dilute Fe-Mn and Fe-Mo Alloys (V.S. Raghunathan and B.D. Sharma)

Self-diffusion studies in a series of dilute iron base alloys having manganese and molybdenum as alloying additions, have been conducted to establish 'correlation effects'. The data have been analysed in accordance with Lidiard's theory. The temperature dependence of diffusivity in these alloys could be represented by the following Arrhenius equations :

Alloys (at%)	Eqn.	Temp. range °C
Fe-1 Mn(γ)	$D = 0.38 \exp(-66,400/RT)$	970-1205
Fe-3 Mn(γ)	$D = 0.08 \exp(-61,400/RT)$	-do-
Fe-1.5Mo(α)	$D = 2.24 \exp(-57,600/RT)$	802-902
Fe-3 Mo (α)	$D = 1.1 \exp(-55,800/RT)$	-do-

The typical values for correlation factor for Mn⁵⁴ and Mo⁹⁹ diffusion in these alloys were characteristic of vacancy diffusion. For example, f_1 for the diffusion of Mn in γ -Fe at 1017°C was 0.78. The same value was obtained for Mo diffusion in α -Fe at 802°C.

(ii) Self and Impurity Diffusion in Dilute Zirconium-base Alloys (R.V. Patil, G.P. Tiwari and B.D. Sharma)

Studies on self- and impurity diffusion in dilute Zr-Cr, Zr-Al, Zr-Fe alloys in beta phase (which shows anomalous diffusion) have been continued.

(iii) Diffusion of Fe⁵⁹ in Concentrated Fe-Al, Fe-Si Solid Solutions (V.S. Raghunathan and B.D. Sharma)

Diffusion of Fe⁵⁹ in Fe concentrated solid solutions in the Fe-Al and Fe-Si systems has been investigated, the points of interest being (i) temperature and composition dependence, (ii) effect of magnetic ordering and (iii) short range order on diffusion behaviour

in these alloys. The following results for temperature dependence were obtained :

<u>Alloy</u>	<u>Diffusivity</u>	<u>Temp. range</u>
Fe-6Al	$D = 0.42 \exp (-42,290/RT)$	(Pure)
Fe-10Al	$D = 0.02 \exp (-43,880/RT)$	(Pure)
	$D = 0.06 \exp (-46,720/RT)$	(Ferro)
Fe-15Al	$D = 0.01 \exp (-41,290/RT)$	(Pure)
	$D = 0.01 \exp (-47,290/RT)$	(Ferro)
Fe-10Si	$D = 0.25 \exp (-55,140/RT)$	(Pure)
	$D = 5.59 \exp (-52,420/RT)$	(Ferro)

The composition dependence of frequency factor in Fe-Al system could be correlated with entropy of mixing for alloys of different compositions. The activation energy could be correlated to alloy compositions through solidus temperatures by an equation :

$$D = D_0 \exp (\phi \cdot S^{\text{mix}}/R) \exp \left[\frac{-Q}{(T_s/T_m)} \right] \exp \left\{ -(K-\phi)n_B \right\}$$

where ϕ and K are proportionality constants.

The studies have also shown that both ferromagnetism and short range order strongly affect diffusion coefficients.

(iv) Chemical Diffusion in bcc Solid Solutions

(a) Fe-V System

(V.S. Raghunathan, B.D. Sharma)

Using electron microprobe analysis, the interdiffusion behaviour in Fe-V system has been investigated in the temperature range 1200-1400°C. Effort was made to rationalise the diffusion data in terms of Vignes-Birchall's treatment correlating D values with solidus temperature, as in the case of Zr-Ti system reported last year. The correlation was found to hold good in the composition range 10-70% Fe. Temperature dependence of interdiffusivity in this (0-70 at% Fe) region is seen to follow the relationship

$$D = 23.4 \exp (-4.6 \text{ Fe}) \exp \left[- (80,800 - 34000 \text{ Fe})/RT \right]$$

Below 1200°C, due to formation of σ phase, the diffusivity data show scatter.

(b) Titanium-Vanadium System

(G.B. Kale, S.K. Khara and G.P. Tiwari)

The chemical diffusion in Ti-V diffusion couples has been investigated in the temperature range 900-1200°C. The concentration profiles obtained by EPMA have been analysed in accordance with Boltzmann's analysis and the data rationalised following Vignes-Birchenall's treatment. Ti-V system shows a minimum in solidus temperature in the 30-40%Ti range. Diffusion coefficients increase with decrease in solidus temperatures. The data do not follow Vignes-Birchenall's treatment monotonically and have been used to establish free energy vs composition diagram.

(v) Phase Stability and Diffusion Controlled Growth of Intermetallic Compounds

(a) Thorium-Iron and Thorium-Stainless Steel Systems

(S.K.Khara, R.V. Patil, B.D. Sharma)

In continuation of the earlier work on Th-V system, the phase stability of thorium-iron compounds in the diffusion zones of Th-Fe and Th-stainless steel couples was taken up for study. While difficulty was experienced in making Th/stainless steel diffusion couples, the results on Th-Fe system have been quite interesting. Diffusion couples equilibrated in the range 690-780°C have shown presence of Th_7Fe_3 , ThFe_3 , ThFe_5 and $\text{Th}_2\text{Fe}_{17}$ intermetallics in the diffusion zone. The relative distribution of these phases is found to vary with temperature and time of anneal. The data have been analysed to obtain the relative growth rates of these intermetallic compounds.

(b) Iron-Titanium System

(G.B.Kale, S.K. Khara and G.P. Tiwari)

The Fe-Ti system, unlike the Ti-V system, does not exhibit

complete solid solubility. The phase diagram exhibits the presence of two intermetallics, i.e. $TiFe_2$ and $TiFe$. Diffusion studies using EPMA are currently in progress to examine the relative distribution, phase stability and the growth rate of these compounds in the diffusion zone of Fe-Ti 'sandwich' couples.

- (vi) Hydrogen Absorption and Hydride Precipitation in Zr-Base Alloys
(M.D. Vora and B.D. Sharma)

The hydrogen absorption characteristics of iodide and sponge zirconium, zircaloy-2, Zr-2.5%Nb and some Zr-Ni alloys have been investigated in the temperature range 275-550°C. Hydrogen absorption is marked by transients attributable to surface effects.

The diffusion controlled transformations accompanying ZrH_2 precipitate formation and dissolution have also been investigated. The data for precipitation follow the well known Johnson-Mehl correlation and yield an activation energy of 8200 cal/gm.mol for hydrogen diffusion in zirconium alloys. Dissolution experiments involving heat treatments of zirconium alloys containing hydride platelets above α/α' (hydride) phase boundary, have also yielded results confirming the above activation energy.

- (vii) Solute Redistribution Studies in Oxidised Zirconium Alloys
(S.K. Khara, G.B. Kale and H.S. Gadiyar)

EPMA studies on solute distribution in oxide layers, and in oxide/metal interface regions, have been conducted for Zircaloy-2 and Zr-binary alloys containing Nb, Cr, Sn, Cu and Ni. The specimens are oxidised in steam at 558°C. In the case of alloys showing higher oxidation rates, the solute oxide is found to dissolve in the ZrO_2 matrix without any composition variation. However, for solute additions of limited solubility like Cr, Ca and Fe, solute enrichment at interface and depletion in the alloy is observed. The results are of interest in relation to the relative stability of various oxides, as also the oxidation behaviour of zirconium alloys.

2.3.2. Neutron Irradiation Effects

(i) Defect Structure and Post-Irradiation Annealing of Neutron Irradiated Nickel Alloys

(M.K. Matta, I.S. Batra and B.D. Sharma)

The defect structure caused by neutron irradiation, which is responsible for radiation hardening, has been examined by transmission electron microscopy in polycrystalline nickel, Ni-Ti and Ni-Fe alloys. The defect structure is found to consist of depleted zones, black-white defects, dislocation loops, vacancy tetrahedra and dislocation tangles of varying sizes and density. The defect density of tetrahedra and dislocation loops is found to be high in Ni-Ti and Ni-Fe alloys as compared to the pure metals. Post-irradiation annealing studies have also shown that radiation hardening, associated with these defects, anneals out in the temperature range 150-300°C, with an activation energy of 2.1 eV. This is lower than the activation energy for self diffusion in pure nickel.

(ii) Solid Solution Strengthening in Nickel Base Alloys

(M.K. Matta and B.D. Sharma)

The mechanical properties of Ni-1%Ti, Ni-5%Ti and Ni-8%Fe alloys have been investigated in the temperature range 77-450°K. These studies have been concerned with tensile strength properties, work-hardening behaviour, evaluation of 'thermal' and 'athermal' components of flow stress and, thermal activation parameters. Intersection of solute-induced 'forest dislocations' has been found to be the rate controlling mechanism in low temperature deformation. Cottrell's elastic interaction appears to be effective in dislocation binding at higher temperatures. TEM has shown ample evidence for large scale dislocation tangles in high concentration alloys.

Portevin-Le Chatelier effect has been observed during tensile testing of Ni-1%Ti alloy in the temperature range 275-450°C at strain rates varying from $2.62 \times 10^{-5} \text{ sec}^{-1}$ to $2.62 \times 10^{-4} \text{ sec}^{-1}$.

The results are quite interesting as these provide evidence for application of the dynamic strain ageing model for serrated yielding in nickel-titanium alloys. The studies yielded an activation energy of 0.99 eV for migration of titanium in nickel.

(iii) Neutron-irradiation Strengthening in Nickel Alloys
(B.D. Sharma and M.K. Matta)

The effect of neutron irradiation on tensile properties of Ni-1%Ti, Ni-5%Ti and Ni-8%Fe alloys has been investigated in the temperature range 77-408°K. Strength parameters, work hardening rates and thermal activation parameters for low temperature deformation of irradiated alloys have been investigated. The irradiation hardening in alloys is found to follow $(\Delta\sigma)_{irr} = (\Delta\sigma)_{scln} + \Delta\sigma_{irr}$ relationship. Analysis of thermally activated deformation parameters has shown short range obstacles of $H_0(\sigma^*) \approx 3.0$ eV to be rate controlling in irradiation strengthening.

(iv) Radiation Hardening in Iodide and Sponge Zirconium
(B.D. Sharma, M.K. Matta and I.S. Batra)

The temperature dependence of flow stress and its strain rate sensitivity have been investigated for iodide and sponge zirconium neutron irradiated to different doses in 1.0×10^{18} n/cm² - 6.5×10^{18} n/cm² range. Studies on unirradiated metals have shown P.N. force to be rate controlling in low temperature deformation of iodide zirconium, and dislocation-pinning by oxygen atoms in the case of sponge zirconium. The effect of neutron irradiation on thermal activation parameters is seen in reduced ΔA^* values with neutron dose for iodide zirconium; there is almost little influence in sponge zirconium.

The dose dependence and temperature dependence of flow stress in irradiated zirconium of both iodide and sponge purity, follow Seeger's hypothesis predicting $(\Delta\sigma)$ vs $(\phi.t)^{1/2}$ and $(\Delta\sigma)^{2/3} \eta T^{2/3}$ relationships.

The effect of neutron irradiation on Hall-Petch relationship for sponge zirconium has also been investigated for different temperatures. Neutron irradiated specimens followed the Hall-Petch equation

for low neutron doses, but at elevated temperatures 'anomalous' results were seen.

- (v) Quench-hardening and Quench Irradiation Hardening in Zircaloy-2 and Zr-1%Al Alloys
(M.K. Matta and I.S. Batra)

The low temperature deformation of as-quenched and quench-irradiated zircaloy-2 and Zr-1% Al alloy has been investigated in the temperature range 77-400°K. The flow stress temperature and strain rate sensitivity studies have been used to evaluate 'thermal' and 'athermal' components, and thermal activation parameters. Though both quenching and irradiation increased yield stress values substantially, the relative changes in activation area values were quite small, suggesting that long range, quenching stresses retained in the matrix have a stronger role to play in the strengthening process. The rate controlling mechanism in low temperature deformation is interstitial-dislocation interaction.

- (vi) Swelling Behaviour of Irradiated Copper Boron Alloys and Growth of Gas Bubbles
(G.P. Tiwari)

The studies on nucleation and growth of gas bubbles in neutron irradiated Cu-Boron alloys have been continued. Metallographic examination has revealed ample evidence concerning various stages of bubble growth. To begin with, bubbles grow individually unaffected by the proximity of neighbours. The next step is growth by coalescence, when neighbouring bubbles join up to form bigger bubbles. The driving force for this type of growth is visualised to be the increase in the entropy of gas present inside the bubbles. The free surface and grain boundaries act as important vacancy sources for the exchange process contributing to this type of microstructure.

- 2.3.3 Solidification Texture in Splat-cooled Alloys
(P.K.K. Nayar)

Studies on solidification textures in splat cooled metals and alloys have been continued. Some interesting results on Al, Bi, C.

Pb and Zn were published during the year. It is to be mentioned that this aspect of aplat cooling has received practically little attention in the past.

2.3.4. Computer Based Research
(S.K. Khara)

A computer programme to facilitate the analyses of SAD patterns from intermetallic compounds of two or three elements has been developed; the programme being applicable to all crystal systems. By using it any zero order laue zone, reciprocal lattice section corresponding to a given structure can be plotted directly by the computer. In addition, the interplanar distances and relativistically corrected values of structure factor and extinction distance for any Bragg reflection can be calculated.

3. CORROSION AND ELECTROMETALLURGY

The Corrosion and Electrometallurgy Section has continued its activities on the development of corrosion resistant materials for high-temperature high-purity water and for sea water applications. Stress corrosion cracking of zirconium alloys in iodine atmosphere, basic studies on corrosion in high-temperature high-purity waters, electroplating of metals and alloys, electroplating of composite materials, electrowinning of cobalt rare earth alloys and hydrometallurgical leaching of metal values from nickel and copper concentrates, formed the active part of the programmes. The Section has also carried out various consultancy services and rendered assistance in failure analysis studies.

3.1 HIGH TEMPERATURE CORROSION STUDIES

3.1.1 Oxidation of Zr-Ni alloys

(H.S. Gadiyar and S. Chakravarty)

In comparison with several Zr-base alloys such as Zr-Nb, Zr-Cr and other alloys, corrosion studies of binary Zr-Ni alloys containing 0.1 to 2.0 wt.% nickel have been carried out in high temperature water at 360°C, steam at 400 and 550°C and oxygen at 600°C. This study will also throw some light on the belief that nickel addition to zirconium alloys would cause considerable acceleration of hydrogen absorption of these alloys. In high-temperature water, early oxide spalling was observed on all the alloys and the hydrogen absorption was nearly 100% of corrosion hydrogen in several cases. The higher the nickel content in the alloy the more was the amount of hydrogen absorbed. This increased hydrogen absorption has been attributed to the metallic surface activity of nickel which gets concentrated at the oxide surface during corrosion. In steam at elevated temperatures, the corrosion rates are low due to a nickel enriched layer near the metal/oxide interface. But again the oxide grown is prone to early spalling. This has been correlated with the distribution of hydrides in the metal matrix and the type of cracks formed at the metal/oxide interface.

3.1.2 Effect of ion implantation on the corrosion resistance of zircaloy-2 (H.S. Gadiyar and S. Chakravarty)

The technique of ion implantation has been recently gaining importance as one of the corrosion preventive measures. Tubular zircaloy-2 specimens were implanted with argon ion at Nuclear Physics Division to have a thin affected layer on the surface. These were corrosion tested in pressurized water at 300°C with a view to assessing the effect of ion implantation. The control specimens showed weight gains of 14 mg/dm² after about 700 hours of exposure while the implanted specimens showed weight gains of about 24 mg/dm². This indicates that in these periods of exposure the effect of ion implantation is not pronounced. Similar results were obtained also in steam at 450°C. Further work is in progress with a view to implanting Fe and/or Cu ions on the surface and testing for the performance of these ion implanted specimens.

3.1.3 Corrosion of zirconium alloys under dynamic conditions (H.S. Gadiyar, S.V. Phadnis and S. Chakravarty)

From the static corrosion studies on a variety of zirconium alloys in water and steam at temperatures from 300 to 500°C, it was earlier shown that additions of Nb, Fe, Cr and Cu as alloying elements to Zr improve the latter's corrosion resistance. To extend the study to dynamic conditions in flowing water, several alloys were exposed in a dynamic corrosion loop containing high temperature water at 550°F, flowing at a rate of 7 - 8 ft./sec at a pressure of 1200 psi. This loop is located at and operated by the Reactor Engineering Division.

Upto a total exposure of 3040 hours, the weight gains obtained on zircaloy-2 and the experimental Zr-0.5 Nb-1Cr alloy are comparable indicating equivalent corrosion resistance under dynamic conditions also. The binary alloys like Zr-Nb and Zr-Cr, however, had higher weight gains than zircaloy-2. The exposures are being continued.

3.1.4 Magnetite coating on mild steel in high temperature water
(H.S. Gadiyar and S. Chakravarty)

It has been shown earlier that a protective magnetite coating forms on mild steel when it is exposed to high temperature water at a pH of 10.5. This work has been continued in order to study the long term stability of the magnetite coating to determine the corrosion product transport to water and to study the effect of dissolved oxygen in water on the protectiveness of the magnetite coating. The initial studies were carried out at a pH of 10.5 and temperature 600°F with 4 ppm of dissolved oxygen. The magnetite formed was adherent and protective and had an average thickness of 1.9 microns. The base metal corrosion rate was high in the beginning and considerably reduced towards the end of about 127 days of exposure. Further experiments are in progress to determine the effect of oxygen in the environment on the protective nature of the coating.

3.2 CORROSION OF ZIRCONIUM ALLOYS IN IODINE ATMOSPHERE

3.2.1 Stress corrosion cracking in iodine vapour
(K. Elayaperumal and G.C. Palit)

It has been reported earlier that annealed zircaloy-2 is susceptible to stress corrosion cracking in methanol - iodine solutions when stressed uniaxially to a level of 75% of 0.2% yield strength. This iodine stress corrosion cracking study has been extended to the actual fuel cladding zircaloy tubes. The RAPP type fuel tubes were obtained from NPC through FPED. Rings cut from these tubes were stressed beyond yield strength either by a tight fitting mandrel or by forcing a wedge on a slot made on the ring. These were exposed to pure iodine vapour at 300°C. The results to-date indicate that stressing either by mandrels or by slotted ring does not lead to cracking even at high concentration of iodine (about 30 mg/dm²). However, in the presence of a catalyst viz. steel wool, the slotted zircaloy rings were found to be embrittled after exposure to iodine. These embrittled specimens could easily be cut by manual bending. Apparently the occurrence of stress

corrosion cracking requires very specific type of stress and localised concentration of iodine. Further experiments are in progress to arrive at the conditions which will lead to cracking, and to examine the crack pattern by microscopy.

3.2.2 General corrosion of zircaloy-2 in iodine
(K. Elayaperumal and G.C. Palit)

Sometime during the middle of the year, it was reported that iodine activity in TAPS reactor water showed a considerable increase above the normal values. With a view to examining the possibility that the general corrosion of zircaloy-2 cladding with fission generated iodine may occur to such an extent to result in excess iodine activity in the reactor water, a programme has been conducted to study the general corrosion of zircaloy-2 tubes in iodine vapour. Weighed zircaloy rings cut from the cladding tube were exposed to iodine vapour at 300°C for a long time. The corrosion products obtained were dissolved in water which was later analysed for zirconium and iodine. The results indicated the following:-

The colour of the solution obtained by just dissolving the corrosion product (pH = 2) was found to be slowly turning to violet indicating the full release of iodine. In the acid solution all the reacted zirconium and iodine end up in the solution whereas in the alkaline solution (pH = 11.5 by adding LiOH), the amount of zirconium was of the order of magnitude less than that in acid solution while iodine remained the same. Since the reactor water is slightly alkaline and the actual reactor water while showing increased activity of iodine did not indicate any appreciable quantity of zirconium, it is possible that corrosion of zircaloy with iodine may also be one of the causes of increased iodine activity in the reactor water.

3.3 CORROSION OF MATERIALS IN SEA WATER AND SAFT WATER CONDITIONS

3.3.1 Corrosion of Al-Mg alloys
(H.S. Gadiyar, N.S.D. Elayathu and V.P. Joshi)

Al base alloys are of interest to desalination applications because of their good thermal conductivity, greater availability and

good corrosion resistance in the neutral pH range. However, their use will involve careful design and engineering particularly to avoid pitting and galvanic corrosion. In this connection, studies on the corrosion behaviour of Al-Mg alloys containing 1.0, 3.5 and 7.0 wt.% Mg have been carried out in ambient and boiling 3.5% NaCl solution. Long term exposures (upto 400 days) at room temperature have indicated low corrosion rates (about 0.1 mpy) and absence of pitting on all the three alloys. In boiling solution, the corrosion rates were higher (1.1 mpy over 200 days for 7% Mg; 1.7 mpy over 544 days for 3.5% Mg and 3.0 mpy over 370 days for 1% Mg alloy). Pitting and crevice effects were predominant on the 1% Mg alloy while they were less severe on the alloys of less Mg content. The results, thus, indicated satisfactory corrosion behaviour of the 7% and 3.5% Mg alloys both in ambient and boiling NaCl solution.

3.3.2 Corrosion of copper and titanium alloys (P.R. Shibad)

In a programme to determine the corrosion characteristics of Cu-base and Ti-base alloys to salt water systems in desalination service, two new materials were tested in the laboratory under conditions representing those existing in desalination systems. These are a Cu-base alloy containing 9% Sn and 2% Al and a Ti-2% Mo alloy. The choice of the two alloys is based on the published informations on sea water corrosion rates of similar alloys. These were tested for 15 days in synthetic sea water and also in 3% NaCl solution and the effect of pH, temperature and stirring has been studied. The results indicated the following:-

Neither pitting nor any other localised attack was seen on the Cu-base alloys. The rates of the Cu-base alloy are generally low and within the normally acceptable limit of 5 mpy. However, the corrosion rate was quite high under acidic conditions which might develop under crevices. Hence, the performance of the Cu-base alloy is not acceptable. The Ti-Mo alloy is very resistant under all the conditions tested. These

laboratory results will be compared later with the results obtained by exposing these specimens to flowing sea water in a loop operated by Reactor Engineering Division in CIRUS jetty.

3.3.3 Corrosion of Cu-Al₂O₃ and Ni-TiO₂ composites in salt water
(P.R. Shibad, M. Totlani and M.N. Joshi)

The composite materials Cu-Al₂O₃ and Ni-TiO₂ were obtained in the laboratory by electroplating of copper and nickel in conventional baths which contained a fine dispersion of alumina or titania particles. In addition to testing their strength, hardness and conductivity, their corrosion resistance in salt and sea water conditions was also studied. Both the 3% NaCl solution and synthetic sea water were used. The results indicated that the corrosion rates of the dispersion hardened composites are not very much different from those of parent metal. The composites were examined metallographically before and after corrosion and it was observed that the interface between the particle and matrix is probably corroding preferentially giving rise to slight weight loss in extreme conditions. It is, thus, seen that the addition of oxides to increase strength does not affect the corrosion resistance appreciably.

3.4 BASIC STUDIES ON CORROSION

3.4.1 Studies on the mechanisms of oxidation of zirconium alloys
(H.S. Gadiyar)

The transition observed during the kinetic studies on corrosion (which generally represents the break-down in the protective nature of the oxide film) has been earlier explained as due to an oxide re-orientation process and development of texture in 202̄ plane. Beneficial effects of Fe, Cr and Cu have been observed during oxidation in high temperature steam environments above 400°C. This aspect has been correlated to the redistribution of the second phase in the oxide layer and metal/oxide interface using electron microprobe analyser. An

enrichment of these alloys has been observed near the Zr/ZrO_2 interface. This acts as a barrier for the decreased corrosion rates.

3.4.2 Effect of environmental nitrogen on high temperature corrosion resistance of zirconium alloys
(H.S. Gadiyar and S.V. Thadnis)

The presence of nitrogen in the environment can cause deleterious effects on the corrosion resistance of zirconium alloys. In this in view, a few zirconium alloys (binaries with Ni, Sn, Cr and Zircaloy-2) were exposed to the commercially pure nitrogen at a temperature of 600°C. It was seen that environment nitrogen accelerated the oxidation of zirconium alloys, zircaloy-2 being particularly affected at this temperature. This effect was found to be less for Zr-1Ni and Zr-1Sn alloys particularly during the initial pre-transition oxidation. The study is being extended to nitrogen - saturated aqueous medium at 360°C.

3.4.3 Prevention of stress corrosion cracking of zircaloy-2 in methanol/iodine solution
(K. Elayaperumal and G.C. Palit)

Annealed zircaloy-2 has been earlier shown to be susceptible to stress corrosion cracking in methanol/iodine solution. Attempts have been made to prevent stress corrosion cracking by adding water as an inhibitor to the methanolic solution. The times to failure of annealed tensile specimens stressed uniaxially to 75% of 0.2% Y.S. in methanol/iodine solution at room temperature have been determined as a function of added water. Complete immunity to SCC was achieved at 15% water. Dynamic stress corrosion tests in a tensile testing machine also indicated the same effect of water. Electrochemical measurements on variation of corrosion potential with time and potentiostatic polarization characteristics indicate that water inhibits the anodic reaction by forming protective passive film.

3.4.4 Stress corrosion cracking of binary Zr-Fe and Zr-Cu alloys
(K. Elayaperumal and G.C. Palit)

In continuation of the earlier reported study on stress corrosion cracking of Zr-Cr alloys, work has been carried out on the stress corrosion cracking of Zr-Fe and Zr-Cu alloys in methanol/HCl solution. It was observed that 2% Fe reduces the corrosion rate and the susceptibility to intergranular stress corrosion cracking of zirconium. Addition of 2% Cu also induces resistance to stress corrosion cracking of zirconium. The resistance offered by Cu is more in degree than that offered by Fe. Unlike Zr-2% Cr alloy, the Zr-2% Fe alloy has no duplex eutectoid structure at the grain boundaries. The intermetallic $ZrFe_2$ globules are distributed at random in alpha phase matrix. This may be the reason why 2% Fe in zirconium does not induce complete resistance to SCC. Further experiments are in progress to explain the different effects of Fe and Cu.

3.4.5 Pitting of zirconium in chloride solutions
(K. Elayaperumal and S.S. Chouthai)

In order to characterise the pitting tendency of zirconium in the presence of chloride ions and to compare this tendency with that of stainless steel, basic electrochemical investigations were carried out on zirconium while exposed to aqueous solutions of chlorides and sulphates. Preliminary results showed that pitting of zirconium occurred in sulphuric acid solutions containing certain amount of chlorides either as HCl or $FeCl_3$ and that addition of oxidising sulphates such as cupric sulphate and ferric sulphate prevented pitting. In the electrochemical studies critical break-down potential in a potentiostatic anodic polarization curve is taken as a measure of the pitting tendency. This was measured as a function of the ratio SO_4^{2-}/Cl^- . The results showed that zirconium is having high pitting tendency in a neutral chloride solution and that addition of sulphate increases the critical pitting potential to more noble values indicating increased resistance to pitting. This is

indicative of the increased stability of the passive film in high sulphate solutions. The exact relation between the chloride ion and the required sulphate ion to prevent pitting is being compared with the one available for stainless steels.

3.4.6 Measurements of pitting tendency on Al-Mg alloys (H.S. Gadiyar and V.P. Joshi)

Electrochemical polarization studies have been carried out on Al-Mg alloys in 3.4% NaCl solution for determining the corrosion potential, breakdown potential and the protection potential against pitting so as to predict the pitting tendency of these alloys in salt water systems. At room temperature, the corrosion potentials were always more active than the protection potential indicating that the alloys are less prone to pitting at these exposures. On the other hand at boiling temperature, the protection potentials were either close to corrosion potentials or even slightly more active showing that the alloys are in the possible pitting region. This corresponds with the simple immersion tests on these alloys which have shown pitting to occur generally at the boiling temperature but not at the room temperature.

3.5 CONSULTANCY SERVICES AND ASSISTANCE

The Section has continued its services in the form of consultancy and assistance to the various units of DAE on corrosion and related problems. Some of these are briefly described below.

3.5.1 Services to PREWAC

The Section is represented in PREWAC (Power Reactor Water Chemistry Group) which undertakes research and development activities in connection with water related problems in the various power stations of DAE. During the year under consideration the following five reports have been sent:-

1. A report on the general corrosion of zircaloy-2 in iodine to explain the reported excess iodine activity in the TAPS reactor water. This report was based on the work carried out in the Section (Please see item 2.2) - (K. Elayaperumal and G.C. Palit).

2. Substitution of nitrogen for helium in EHT storage tank of RAPS-I : Corrosion aspects - (H.S. Gadiyar).

3. Corrosion of carbon steel in high purity high temperature water in relation to dissolved oxygen - A literature survey (H.S. Gadiyar).

4. Two summary reports on "Curing Condenser Tube Corrosion by Ferrous Sulphate Treatment" (K. Elayaperumal).

3.5.2 Inhibition of carbon steel corrosion in fresh water
(K. Elayaperumal, H.S. Gadiyar and S. Chakravarty)

In continuation of the failure analysis studies of a carbon steel heat exchanger tube used in service in a fresh water cooler, reported earlier, studies have been carried out to find a suitable inhibitor for prevention of corrosion of carbon steel in flowing fresh water. Attempts were concentrated on finding a suitable non-toxic, non-foaming inhibitor which can be separately handled in fresh water systems. By accelerated laboratory test, it has been found that a mixture of zinc sulphate, sodium di hydrogen phosphate and sulphamic acid is effective in reducing the corrosion rate by about 99% at a total concentration of 60 ppm.

3.5.3 Intergranular corrosion testing of Type 316L S.S.
(K. Elayaperumal and V.P. Joshi)

In response to a request from an Engineering firm in Bombay, a set of investigations was carried out in order to check the intergranular corrosion susceptibility of Type 316L S.S. with which the firm was fabricating an equipment for manufacture of chemicals. The tests were carried out according to the standard ASTM specifications. The supplied steel was found not to be susceptible to intergranular corrosion.

3.5.4 Metallographic testing of Cupro-nickel tubes
(K. Elayaperumal and V.P. Joshi)

In response to a request from a Petrochemical organisation, cupro nickel tubes of composition 70 Cu-30 Ni were metallographically examined to determine whether the tubes were in the annealed condition or in the cold rolled condition. The examination revealed that the tubes were partly annealed.

3.5.5 Corrosion testing on Monel tubes
(H.S. Gadiyar)

Some accelerated corrosion tests were carried out on Monel tubes received from Atomic Fuels Division. These tubes had some scratches on the outside surfaces introduced inadvertently during fabrication. The tests were carried out in order to see whether these scratches affect the corrosion behaviour. The test environment was distilled water containing 500 ppm chloride at a temperature of 310°C and under pressure of 1430 psi and the period of exposure was 45 days. Examination of the corroded specimens indicated that the corrosion was uniform through-out and that the scratches had not affected the corrosion behaviour.

3.5.6 Chromium plating on the metallic seal of R-5 guide tube
(A.K. Grover)

In response to a request from R-5, preliminary work on chromium plating was done on Type 304 SS plates prior to actual plating on the metallic seal of R-5 guide tube. The latter is likely to rub continuously against the lattice tube because of thermal expansion or contraction. It should have good wear resistance and hence chromium plating was attempted. Adherent hard chromium deposit was obtained in the preliminary tests. The hardness of the deposit ranged from Rc 45 to 50. A total of nine metallic seals has been plated and sent to Reactor Engineering Division for testing their suitability as wear resistant coating.

3.5.7 Supply of rare earth metals
(Sohan Singh and A.L. Pappachan)

The individual rare earth metals like cerium and lanthanum and also the mixtures of lighter rare earth metals, misch metal, have been supplied in response to requests from various research organisations in batches of 1 or 2 Kgs. for research purposes.

3.6 HYDROMETALLURGICAL EXTRACTION OF METALS

3.6.1 Nickel from Jaduguda concentrates
(M. Totlani, P.R. Singh and S.N. Athavale)

It has been earlier observed in the test on acid pressure leaching that grinding the copper nickel concentrates to finer mesh (greater than 99% -325 mesh) enhances the leaching rate at the oxygen over pressure of 500 psi. It may be possible to reduce this oxygen over pressure with the concentrates still finer (greater than 99% -400 mesh), thus relaxing the requirement of high pressure in the material of construction. Systematic grinding tests were carried out with the copper nickel concentrates which was only 16% - 200 mesh. On a scale consisting of 500 gms of the concentrate (100% -400 mesh), it was possible to get complete nickel recovery by leaching at an oxygen over pressure of only 160 to 180 psi at a temperature of 230°F. Systematic tests are in progress to study the suitability of process.

3.6.2 Fluidized bed electrolysis
(M. Totlani and P.R. Singh)

A programme on the use of fluidized bed electrode in the recovery of nickel from dilute leach liquors consisting of nickel sulphate has been taken up. Due to the improved surface area to volume ratio, this system has advantage over the conventional electrolytic process particularly in the case of dilute solutions through the absence of concentration polarization. The fluidized bed was made of nickel powder of 60 micron size. The preliminary experiments have

shown that total output current is maximum at a bed expansion of 9 to 12%. With higher fluidization, there is reduction of current due to the loss of electrical continuity through the particles. Further work is in progress to electrodeposit nickel from the leach liquors.

3.6.3 Tungsten from scheelite concentrates (M. Totiani, P.R. Singh and A. Ramasamy)

Studies on the extraction of tungsten values from low grade scheelite concentrates of the Kolar Gold Field have been continued. A WO_3 recovery of over 95% has been achieved by following the decomposition of the concentrate on a 100 gms scale with sodium carbonate in presence of silica at a temperature of 750 to 760°C for 4 hours. Investigations have also been carried out to separate WO_3 by a two phase extraction in molten state using soluble halide phase and insoluble alumina-silica phase. A maximum of 50% WO_3 extraction in the halide phase has been achieved at a temperature of 1080°C from a charge containing 150 gms. of scheelite concentrates.

Studies on the preparation of fine tungsten powder by hydrogen reduction of WO_3 have been completed. It was possible to obtain in the laboratory very fine tungsten powder with an average particle size of 0.3 micron by following the hydrogen reduction in the presence of hexamine (10 to 12%) at a temperature of 750 to 800°C.

3.7 ELECTROWINNING OF RARE EARTH METALS

3.7.1 Electrowinning of lanthanum (Sohan Singh and A.L. Pappachan)

Programme on the electrolytic preparation of individual rare earth metals has been continued. Lanthanum metal has been prepared by fused salt electrolysis from a chloride bath, (40% lanthanum chloride in KCl - NaCl eutectic) at 960 to 970°C. The maximum current efficiency was 86% at a current density of 8.25 amp/dm². The metal obtained was of purity better than 97%, the major impurity being iron.

3.7.2 Preparation of cobalt-cerium permanent magnet alloys
(Sohan Singh and A.L. Pappachan)

Permanent magnets consisting of alloys of cobalt with various rare earth metals are several times superior to the conventional Alnico type magnets in their resistance to demagnetisation. Work has been initiated for preparation of cobalt-cerium alloy from fused rare earth chloride bath with cobalt cathode in a NaCl-KCl eutectic bath at a temperature of 960 to 970°C. Cobalt-cerium alloys have been obtained in the molten state at the cathode and collected in alumina crucibles. It was possible to directly obtain cobalt-cerium alloys with 46.3% cobalt. The alloys so formed was crushed to micron size and is being used for magnetic studies. Further work is in progress to achieve the right composition of the type Co_5R by adjusting the geometry of the cathode, temperature of operation and other electrolysis parameters.

3.8 ELECTROPLATING OF METALS AND ALLOYS

3.8.1 Electroplating of boron free nickel
(P.G. Deshpande)

Electroplating of nickel is usually done from standard Watt's bath containing nickel sulphate, nickel chloride and boric acid. Due to boric acid in solution, the nickel deposits contained traces of boron as impurity. Since boron has high neutron absorption cross-section, it is an undesirable element when electroplated nickel has to be used in reactor structural parts. So a new bath has been developed to get nickel electroplates containing nickel sulphate (300 to 350 gms/l), Aluminium chloride (10 to 15 gms/l) and ortho phosphoric acid (40%), keeping the pH below 4. Thick nickel electroplates (40 mils) were obtained and found to be quite ductile and could be easily cold rolled to about 75% reduction in thickness.

It is planned to use this bath to get nickel/nickel oxide composites for MHD programmes.

3.8.2 Electroplating of Cobalt manganese alloys from fluoborate bath

(A.K. Grover and John T. John)

In continuation of studies on alloy deposition from fluoborate bath, the deposition of cobalt-manganese alloys has been taken up. This alloy has excellent resistance to wear and to high temperature oxidation. In addition to studying the usual plating parameters, the effects of addition agents like ammonium selenate, glycine and citric acid were also studied. A bath of composition 20 wt.% Mn, Co+Mn 20 gm/l and containing glycine, citric acid and sodium lauryl sulphate as anti-pit agent gave the best results if operated at pH 3, temperature 50°C and current density 8 to 16 amp/dm². The maximum Mn content of the alloy was 11%. It was possible to electroplate alloy deposits having thickness greater than 20 microns. The alloy deposits are being evaluated for structure and properties.

3.8.3 Electroplating of composites

(M. Totlani, A. Ramasamy and M.N. Joshi)

Electrodeposited composite coatings are produced when insoluble materials in fine powder form are kept in suspension in the electroplating solutions and the electro-deposition is carried out in the usual way. Inclusion of fine particles in the electrodeposit makes it possible to produce coating with modified mechanical properties and wear and abrasion resistance. Studies have been taken up to investigate the electrodeposition of Cu-Al₂O₃ and Ni-TiO₂ composites and to study their properties.

(a) Copper-Alumina

Copper-alumina electrodeposits are obtained from conventional copper sulphate bath containing alumina particles (0.3 micron) kept in suspension by mechanical stirring. The micro hardness of the deposits increases from 47 VHN for pure copper deposit to 132 VHN for composite deposits containing 2.92 wt.% Al₂O₃. The presence of the second phase

alumina in the copper matrix does not seriously degrade its electrical conductivity. Microscopic examination of the deposit revealed homogeneous dispersion of alumina in the copper matrix. Corrosion properties of these deposits in sea water are being studied.

(b) Nickel-Titania

Nickel-titania electrodeposits have been prepared from the conventional Watt's bath containing titania particles of size 1 micron in fine suspension. The TiO_2 content of the deposit increases from 2.95 to 5.36 wt.% with the increase of TiO_2 in the bath from 25 gms/l to 100 gms/l; the corresponding microhardness increases from 195 VHN to 321 VHN. Oxidation resistance of Ni- TiO_2 deposits vacuum annealed at 650°C for 1 hour, has been observed to be about 30% better than pure nickel electrodeposits. Corrosion properties of these deposits in various media are being evaluated.

3.9 PREPARATION OF ULTRAPURE ALUMINA, SILICA AND YTRIA

(P.G. Deshpande)

Research and Development work has been undertaken to prepare sub-micron grade ultrapure alumina, silica and yttria required for use in electronic industries. Ultrapure alumina (99.999%) has been produced in the laboratory by treating either impure alumina or commercial aluminium metal. The impurities are eliminated as volatile chlorides either by passing dry, pure HCl gas or HCl and 2 to 3% HF gas to obtain the desired purity range. This work is being done in collaboration with Chemistry Division. The ultrapure alumina thus produced has been pelletised at 1500 to 2000 psi pressure and sintered at 1000 to 1400°C. Their electrical properties are being tested in order to check their suitability as insulators.

4. CERAMICS

The Ceramics Section is engaged in Research and Development activities on (1) nuclear ceramic materials e.g. UO_2 , ThO_2 , UC , BeO and Boron Carbide, (2) refractory ceramic materials e.g. Alumina, Mullite, Zirconia, Zircon and magnesia and (3) electrical ceramic materials (barium-titanate capacitor and Ni-Zn-Ferrite bodies and high alumina substrates). The Section also fabricates and supplies to different users in BARC, such refractory ware as crucibles, boats, trays etc., of high alumina and zirconia; and calcium fluoride crucibles to the requirement of the Plutonium Plant.

In the investigations carried out on Nuclear Ceramic materials as UO_2 and BeO , the factors such as powder properties and sintering cycles that influence the sintering behaviour and resultant microstructure were established. A method of evaluating the surface activity and sinterability of UO_2 powders by the surface adsorption of radioactive isotopes such as Mn^{54} and Nb^{85} from solutions, was successfully developed. A method of improving the compactability and eliminating the tendency to pyrophoricity of lower temperature calcined highly sinterable powders of UO_2 , was developed. The method consists of exposing the powders for a short duration at temperatures between 900° to $1000^\circ C$ for 1 to 2 minutes. In the development work on high alumina bodies, a 95% Alumina body was successfully developed having good refractory and electrical insulating properties. Mullite bodies were developed which sinter to imperviousness at temperatures in the range 1400° to $1500^\circ C$. In the studies on barium titanate and Ni-Zn-Ferrite bodies, the influence of fabrication parameters and sintering treatments on densification, microstructure and electrical properties has been established.

4.1. NUCLEAR CERAMIC MATERIALS:

4.1.1 Studies on UO_2

Studies on the development of microstructure in sintered UO_2
(N.S. Anandan and S.V.K. Rao)

An extensive investigation on the sintering behaviour of ADU derived UO_2 powders and the factors that influence the microstructure of sintered UO_2 pellets was completed. In these studies, UO_2 powders were derived for ADU at temperatures ranging from 400° to $1500^\circ C$, and the influence of various sintering cycles and minor additions such as TiO_2 and V_2O_5 on densification and resultant microstructure was investigated. The major findings were:

- (i) The sinterability of the powders decreases as the calcination temperature increases.
- (ii) In the case of active powders, there is an optimum sintering temperature for each powder for attaining highest density.
- (iii) At lower sintering temperatures, porosity is heterogeneously distributed around the grains, and at higher sintering temperatures, as the grain growth proceeds, more of the porosity gets trapped within the grains.
- (iv) There is no change in the microstructure of sintered pellets when reheated for long soaking periods at temperatures lower than the original sintering temperatures; however, reheating to temperatures higher than the original sintering temperatures causes a significant increase in the grain size.
- (v) It is possible to control the grain size in sintered pellets by minor additions such as TiO_2 or V_2O_5 , some acting as graingrowth promoters and some as inhibitors.

It is thus possible to prepare sintered UO_2 pellets to a stipulated density and microstructure by a judicious selection of calcination temperature and sintering cycle, and minor additions where permissible.

Based on the experience gained in the above studies, a new programme has been taken up to study the dimensional and microstructural stability of high density sintered UO_2 pellets when subjected to refiring treatment at $1700^\circ C$ and above, for prolonged soaking periods. These studies will be useful in analysing the problem of in-situ densification of fuel pellets, as reported in some of the American PWR'S and BWR'S, and also in arriving at the parameters to be controlled in the manufacture of UO_2 pellets to attain more stable structures and dimensions.

Studies on characterisation of UO_2 powders.

(G.P. Tiwari, N.G. Soni and S.V.K. Rao)

In an effort to develop new methods for characterising UO_2 powders for their sinterability, the adsorption behaviour of UO_2 powders in adsorbing radioactive isotopes such as Mn^{54} or Nb^{95} from solutions was investigated. It was found that as the calcination temperatures of the powders was increased from 500° to $1400^\circ C$, the amount of adsorption decreased sharply, particularly in the calcination temperature range of 800° to $1000^\circ C$. This is in agreement with the findings that, as the calcination temperature is increased, the sinterability decreases. The sensitivity of this method is being further examined with respect to identifying the variation in the activity of powders from batch to batch - which have been manufactured under seemingly similar conditions but which exhibit variation in their sinterability.

In the characterisation of UO_2 powders, the relation between the morphology of ammonium diuranate (ADU) precipitates on the morphology and sinterability of UO_2 powders derived from them, has been taken up for study. Experiments were aimed at preparing ADU powders of differing morphology by varying the conditions of precipitation. First a saturated solution of uranyl nitrate was prepared by dissolving 800 gms of U_3O_8 in about a litre of HNO_3 (1:1). The pH of the solution was then gradually

raised by the addition of dil NH_4OH (1:1) with continuous stirring and keeping the solution at 60°C . The first batch of the precipitate that formed around pH 2.5 was filtered and collected. Subsequently, further samples were collected in the pH range 2.5 to 4.5 and 4.5 and above. Another sample of ADU was prepared by carrying out the entire precipitation in one operation. A separate sample of ADU was prepared under conditions similar to those adopted at NFC i.e., precipitation from a solution containing 100 gm of uranium ions per litre at 60°C , using dil NH_4OH as precipitant. The morphology of all these ADU sample precipitates after drying is being investigated by Scanning Electron Microscopy.

Studies on flash-heating of UO_2 powders.

(N.C. Soni)

The investigations on the influence of flash-heating treatments on the powder characteristics and sintering behaviour of UO_2 were completed. It is known that, the lower the temperature of derivation of UO_2 from ADU, the greater is the sinterability. Powders derived at lower temperatures exhibit higher specific surface area, poorer crystallinity and greater sinterability but suffer from the drawback of pyrophoricity and poor compactability. In this work, UO_2 powders were prepared from ADU by reduction at 500°C and flash-heated at temperatures from 900°C to 1400°C for short durations. The best results were obtained at flash-heating temperatures in the range 900°C to 1000°C for 1 minute. It is observed that by flash-heating, (i) the powder density as weight per unit volume increases, (ii) the surface area decreases (iii) surface oxidation at room temperature is minimised (the D.T.A oxidation profile shows a gradual increase in temperature of U_3O_7 formation with the increase in temperature and time of flash-heating) (iv) the poor crystallinity of the original powders is retained as revealed by X-ray diffraction patterns, (v) the sinterability is preserved and (vi) the compacting behaviour is improved. It is also observed that by flash-heating, the optimum sintering temperature range is widened which is a very beneficial factor in sintering the pellets in a production scale, as the rejections due to overfiring or underfiring become less.

Studies on electrical conductivity of sintered UO_2
(P.K. Agnihotri and P.V. George)

As minor additions are known to influence the sintering behaviour of UO_2 , a wider range of additions consisting of both metal and metal oxides was chosen and incorporated in UO_2 derived from ADU at $600^\circ C$ in amounts from 0.01 to 0.1 wt%. These consisted of fine powders of Ta, Zr, Ti, Mo, Al, Cr and Nb_2O_5 and TiO_2 . The cold-pressed compacts of UO_2 with the respective additions were sintered in hydrogen atmosphere at $1500^\circ C$ for 2 hours. The sintered densities and electrical conductivity values of all the specimens were determined. It was observed that the conductivity was significantly influenced to different extents with different additions. Additions such as Ti, Ta, TiO_2 and Nb_2O_5 caused a substantial decrease in conductivity whereas a significant increase was observed in the case of Cr additions. The distribution of the minor additions in the structure - whether it is uniform or segregated around the grain boundaries - is being investigated by Electron Microprobe analysis to evaluate the mechanism by which the conductivity is influenced.

The influence of non-stoichiometry on the electrical conductivity of sintered UO_2 is being investigated. For this, 92% T.D. UO_2 pellets were first fabricated from the $600^\circ C$ reduced UO_2 powders from ADU by sintering at $1500^\circ C$ for 2 hrs. These were then refired at $1400^\circ C$ for 1 hour in different atmospheres as purified hydrogen, mixture of argon and hydrogen, argon, mixture of argon and air, and in vacuum, to create different extents of nonstoichiometry. Representative samples of refired pellets are being analysed for O/U ratios and the photo micrographs of the corresponding sintered specimens were taken. The electrical conductivity values of the samples refired in different atmospheres were determined and the values obtained ranged from 5.7×10^{-5} to 4.9×10^{-3} . These are being correlated with O/U ratios and structural changes.

4.1.2. Sintering studies on Beryllia.

(R.Bhat)

The influence of minor additions on the sintering behaviour of beryllia was investigated. To the hydroxide derived BeO powder, additions of MgO, TiO₂ and Fe₂O₃ were incorporated separately in amounts ranging from 0.1 to 1 wt%. Fe₂O₃ was found to be most effective in promoting densification and further in vacuum sinterings at 1500°C, it was observed that it can be substantially eliminated from the system. Pellets with 1 wt% Fe₂O₃ sintered to a density of 94% theoretical at 1400°C for 2 hours in air. Such pellets were taken and re-sintered at 1475°C in vacuum for soaking periods varied from 1 to 32 hrs. By re-sintering, the density was found to increase to 96% theoretical. Chemical analysis of such pellets revealed that the original 1 wt% Fe₂O₃ content decreased to 0.5% at the end of 1 hour soaking and in the next 15 hrs. of soaking, the amount decreased to 0.5 wt%. When the BeO pellets with the 1 wt% Fe₂O₃ were directly sintered at 1500°C in vacuum for different soaking periods, it was observed that with 1 hr soaking, the Fe₂O₃ content decreased to 0.37 wt%, and further to 0.06 wt% at the end of 16 hrs soaking. The evaporation of iron oxide was found to depend upon the order of vacuum, temperature, soaking time and the size of the compact.

The decomposition behaviour of some of the beryllium compounds such as beryllium sulphate and hydroxide was studied by TGA and DTA methods in vacuum and air at temperatures upto 1000°C. Air calcination of Be(OH)₂ showed a progressive loss of weight right from room temperature onwards indicating loss of associated water. The decomposition started at 180°C and was complete at 295°C. Further loss of weight observed between 700° to 900°C was attributed to the decomposition of residual sulphate present (as the hydroxide had been prepared by precipitation with ammonia from beryllium sulphate solution.) In a vacuum of 1.5×10^{-3} Torr, the decomposition was found to shift to a lower temperature range of 105°C to 225°C.

Beryllium sulphate was observed to lose water from room temperature onwards upto 225°C, where all the four molecules of water of crystallisation were removed. The decomposition of this salt started at 700°C and was complete at 890°C. In the case of vacuum, the decomposition was completed at 825°C. Both the compounds of hydroxide and sulphate showed endothermic peaks in DTA at the stages of water molecule removal and decomposition.

X-ray diffraction studies were carried out to determine the crystallite size and growth in case of pure BeO powders as well as those with 1 wt% addition of MgO, TiO₂ and Fe₂O₃ when calcined at 900°, 1000° and 1100°C. It was observed that the crystallite growth is more significantly influenced by the presence of MgO as a minor addition. Also, the influence of minor addition on the crystallite growth was not significant in the 900°C calcined powders and as the calcination temperature increased, the difference decreased except in the case of MgO addition.

4.1.3 Studies on boron carbide (B.D. Zope)

Studies on the development of high density boron carbide which is considered for use as control rod material for FBTR and R-5 Reactors are being carried out. In these studies, the cold pressing and sintering of boron carbide powder as such and with additives such as aluminium, alumina, silica and copper (in amounts of 1 to 5 wt%) was tried out. Both boron carbide powder prepared in the Division by carbothermic reduction and an imported sample of the carbide powder (E.Merck) were used in these investigations. It was found that by vacuum sintering at temperatures upto even as high as 2100°C the densities attained were not more than 75% T.D. When hot-pressings were carried out, it was found that in pressings at temperatures upto 1600°C, no densification had occurred. Hot pressings at higher temperatures will be carried out when the unit becomes available for this work.

4.1.4 Studies on mechanism of sintering

(G.E. Prasad)

The studies on the crystallinity and sintering behaviour of magnesia powders from hydroxide and oxalate were continued using X-ray and electron microscopy. X-ray diffraction analysis revealed that when the hydroxide is calcined at 400°C, the powder is amorphous and crystallinity is gradually developed as the calcination temperature is increased. In the case of oxalate, the oxide derived even at 400°C was found to be crystalline.

Cold compacted pellets of MgO derived from hydroxide and oxalate by calcination at 800°C were sintered at temperatures from 900° to 1400°C. For comparison, pellets from fused magnesia powders were also sintered along with the above. It was noticed that in the case of samples from hydroxide powders, shrinkage started right from 1000°C onwards, whereas those from oxalate started showing shrinkage only at 1300°C. Samples from fused magnesia however, showed no shrinkage in this temperature range.

The topographical features of all those sintered pellets were studied under the scanning electron microscope. The results showed that the nucleation and grain development started from 1100°C in the case of samples from hydroxide and at 1300°C in the case of those from oxalate. These results substantiate the earlier findings that material movement and sintering is faster in the case of amorphous powders compared to those that are more crystalline.

4.2 STUDIES ON REFRACTORY CERAMIC MATERIALS

4.2.1. Studies on Al_2O_3

(S.K. Roy)

Studies on the development of high alumina ceramics were continued. The programme consisted of developing sintered compositions suitable for certain refractory and electrical applications. These compositions have alpha-alumina or corundum as the principal crystalline phase and

are bonded by a limited quantity of alkaline-earth aluminosilicate glassy phase. The alkaline-earth materials chosen were carbonates of magnesium and calcium. The alumina content of the compositions under study is in the range of 92 to 96.0 per cent by weight.

Such compositions get sintered in the presence of a liquid phase under non-equilibrium conditions and therefore the liquid phase exercises considerable influence on the properties and behaviour of the sintered product. The distribution and interactions of the crystalline and the liquid phases in relation to the nature and amount of the liquid phase were studied using model systems. One such system consisted of alpha-alumina and magnesium fluoride as the component materials. A series of sinterings in air were conducted. Microstructural evaluations are being carried out.

4.2.2. Studies on MgO (C.M. Pathak)

The studies on the influence of the morphology of magnesia powders on the sintering behaviour were continued. It is generally considered that the morphology of the pores in green pellets depends to a large extent on the morphology and particle size of the powders used. In these studies magnesia powders of differing morphology were prepared by calcination of parent compounds as magnesium hydroxide, carbonate and tannate. These were cold-pressed and the relative difference in the initial morphology of the pores in the compacts and thereon the progressive changes in the pore morphology during the earlier stages of sintering are being investigated by scanning electron microscopy.

4.2.3. The development of Al_2O_3 and MgO Ceramics for MHD (S.K. Roy and C.M. Pathak)

A development programme has been undertaken of refractories required for the construction of an experimental tunnel module for

the proposed MID studies by the MHD group. The refractory side walls are also required to be electrically insulating.

In view of the extremely high temperatures involved, ceramic materials are considered most suitable. Out of these, alumina and magnesia are identified and these are required to be fabricated to certain given geometrical shapes and sintered at high temperatures around 1600° to 1700°C. Alumina and magnesia powders derived by low temperature calcination of suitable parent compounds, no doubt yield highly sinterable powders but they would pose a problem of excessive shrinkage during sintering. Hence, it was thought desirable to base these bodies on fused alumina and fused magnesia as the starting materials. Also in the case of magnesia, fused magnesia eliminates the problem of hydration during slip casting. Trial bodies have been compounded in which different amounts of active (lower temperature calcined) oxides are added to the fused oxides to enhance the sinterability and at the same time to keep the shrinkages within reasonable limits. Trial samples having shapes similar to the final shapes that are required were made by slip casting as well as tamping methods. These were dried and biscuit fired and finished. The finished pieces are being refired to a temperature of 1600°C in the gas fired furnace. The ultimate shrinkage values by firing at 1600°C are taken as the basis for making the final moulds to fabricate the regular pieces required. This work is in progress.

4.2.4. Studies on the development of Mullite bodies

(Pransh Das and A.K. Kulkarni)

In the programmes on the development of impervious mullite bodies, the relation between calcination treatments and formation of mullite in clay-alumina mixtures has been studied. The influence of repeated calcination and grinding of mixtures calcined at temperatures from 1200°C - 1500°C for $\frac{1}{2}$ hour to 4 hours duration was investigated to find out the conditions under which the

formation of mullite phase is enhanced. Minor additions of $MgCO_3$ were made in some of the trials. It was found that mixtures repeatedly calcined at $1500^\circ C$ and ground attained bulk densities over 95% T.D. when sintered at $1500^\circ C$. It is found that for MgO to act as an aid in attaining imperviousness, the addition of $MgCO_3$ to the batch is required to be made upto 2.5 wt%. However, when the batches with such addition are given a higher calcination treatment (1400° to $1500^\circ C/8$ hrs) and sintered at a higher temperature of $1500^\circ C$, bloating occurred in the pellets with a decrease in bulk density. When the sintering temperature is kept at $1400^\circ C$ with 8 hours soaking, densities of the order of 95% could be attained. X-ray diffraction studies revealed that MgO not only aids densification, but also enhances the amount of formation of mullite phase.

4.2.5 Studies on stabilisation of Zirconia (P.Y. Dalvi)

Detailed investigations have been carried out - using X-ray diffraction techniques - to study the influence of amount of CaO addition and calcination temperature on the per centage conversion of zirconia from the monoclinic phase to the cubic phase. With 0.2 wt% CaO addition and calcination at $1600^\circ C$, the cubic phase formed amounted to 6%. With 0.5 to 0.75 wt% CaO , and calcination at $1200^\circ C$, the conversion was 6-9%, and at $1600^\circ C$ the conversion was 7-11%. With 5 wt% CaO addition, conversion to the extent of 12% was achieved at $1000^\circ C$, which increased to 94% at $1200^\circ C$, 98% at $1400^\circ C$ and 100% at $1600^\circ C$.

4.2.6 Development of Alumina catalyst carriers (G.T. Kamat)

Studies on the development of high surface area porous spheres of alumina to serve as catalyst carriers for the ignition of liquid propellents (hydrazine), as required in the space programs were continued. Trial samples developed in the earlier work, based on alumina derived from aluminium hydroxide were tested and found

to conform to the specifications, except that they showed delayed ignition. In view of this, an alternative method has been developed in which ammonium alum was taken and decomposed at 1000°C yielding alumina having specific surface area as high as 350 m²/gm. To this, 30 wt% Al(OH)₃ was added intimately mixed, pelletised and sintered at 1200°C for 1 hour. The sintered pellets were found to have an open porosity of 5% and a specific surface area of about 250 m²/gm and thereby would meet the specifications. These are under evaluation for their ignition performance.

4.2.7 Development of high alumina substrates (D.D. Upadhyaya and A.K. Kulkarni)

The original high alumina (95%) batch containing 90 parts china clay, 10 parts alumina and 2.5 parts MgCO₃ sinters to imperviousness at 1500°C, whereas at 1400°C a prolonged soaking period is required to achieve the same result. As it is intended to keep the sintering temperature at less than 1500°C, various additions to the batch composition were tried to improve sinterability. When TiO₂ is incorporated to the extent of 2 wt% on the total batch, imperviousness could be attained at 1400°C with 8 hours soaking. The observation on the other additions tried as steatite (3MgO.4SiO₂.4H₂O), CaF₂, LiCO₃ was that they could not influence to the extent TiO₂ could. As there are applications for which even 90% alumina substrates are adequate, trials were carried out on developing this body. A batch composition containing 90 parts Alumina, 10 parts Pyrophyllite (Al₂O₃.4SiO₂.H₂O), 2.5 parts MgCO₃ and 2 wt% TiO₂ was found to sinter to imperviousness at 1400°C/8 hours with a smooth surface.

4.3. ELECTRICAL CERAMIC MATERIALS

4.3.1 Studies on Ni-Zn-Ferrites

(Ram Prasad)

Hysteresis studies were conducted on ferrite samples of Ni_{0.3}Zn_{0.7}Fe₂O₄ composition. These samples were prepared under different sintering conditions and had varying initial permeabilities ranging from 360 to 2050. The tests were conducted at room temperature

and also at lower temperatures down to 4.2°K. It was observed that the coercive force gradually decreased from 4.5 Oe (for sample with initial permeability $\mu_i = 360$) to 0.3 Oe (for sample with $\mu_i = 2050$) as the permeability increased. The relative remanence also decreased from 0.5 to 0.33 in the same range. As the temperature was decreased, an increase in relative remanence and coercive force was observed. At -196°C, the low permeability sample ($\mu_i = 360$) showed a coercive force of 9.8 Oe as compared to 1.5 Oe for high permeability sample ($\mu_i = 2050$). The changes observed in relative remanence and coercive force values with temperature indicate a predominantly single domain behaviour in the low permeability range and a possibility of superparamagnetic behaviour in the case of sample with high permeability.

4.3.2 Studies on Barium Titanate.

(K. Thiagarajan)

Extensive studies were carried out on barium titanate prepared by the direct calcination of the parent compound barium titanate tetrahydrate. These investigations which essentially were aimed at correlating microstructure and dielectric properties involved (i) the hot-pressing of barium titanate, (ii) the effect for external D.C. bias field to arrest some of the induced polarisations in the direction of the field, (iii) the temperature variation of dielectric properties to study the phase transformation from tetragonal to cubic and (iv) high angle x-ray diffraction to evaluate internal stresses due to incomplete phase transformation. From these studies it could be concluded that the grain boundary has a predominant effect on dielectric properties when the surface to volume (of the grain) ratio is very high.

4.4. CERAMIC FABRICATION

(B.D. Zope)

For the fabrication of beryllia crucibles based on the development work earlier carried out, a beryllia lab for slip-casting, pressing and sintering operations is being exclusively set up.

The Ceramics Section has also been fabricating and supplying refractory items as crucibles, boats etc., to different users in BARC, including Calcium Fluoride crucibles for the Plutonium Plant.

LIST OF PAPERS PUBLISHED/ACCEPTED/COMMUNICATED/
PRESENTED FOR PUBLICATION DURING THE YEAR 1975

1. Preparation of Cu-Be alloys from Indian beryl:
C.M. Paul, B.P. Sharma, M.G. Rajadhyaksha, and C.V. Sundaram
Trans. IIM (in press)
2. Production of tantalum metal by the aluminothermic reduction of tantalum pentoxide:
K.U. Nair, T.K. Mukherjee, and C.K. Gupta
J. Less-Common Metals, 41(1975), 87-95
3. Design and application of a high-temperature high-vacuum laboratory induction furnace:
T.K. Mukherjee, G.R. Kamat, and C.K. Gupta
Trans. IIM, Vol. 28, No.3, Jan. 1975, 273-276
4. Recovery of nickel from nichrome scrap:
K.U. Nair, and D.K. Bose
Trans. IIM, Vol. 28, No.4, Aug. 1975, 289-292
5. Electrolytic recovery of molybdenum from molybdic oxide and molybdenum sesquisulphide:
A.K. Suri, and C.K. Gupta
Met. Trans. Vol. 6B, Sept. 1975, 453-456
6. Carbothermic reduction of refractory metal oxides:
S.P. Garg, R. Venkataramani, and C.V. Sundaram
Trans. IIM, Vol. 28, No.4, Aug. 1975, 281-288
7. Thermodynamics of sacrificial de-oxidation of refractory metals:
S.P. Garg, and C.V. Sundaram
BARC Report, 777
8. Thermodynamics of carbon de-oxidation and aluminium de-oxidation:
S.P. Garg, and C.V. Sundaram
Communicated for publication in Met. Trans.
9. Thermodynamic study of Al-Mg system by vapour pressure measurement:
Y.J. Bhatt, S.P. Garg, and C.V. Sundaram
Accepted for publication in Met. Trans.
10. Thermodynamics of Ti-O-O system:
J.M. Juneja, Y.J. Bhatt, and S.P. Garg
Presented at the 6th DAE Materials Science Symposium on
'Phase Transformation and Phase Equilibria' held at Bangalore,
Oct. '75

11. Decomposition of zircon by soda ash sintering process:
P.R. Menon, J.M. Juneja and T.S. Krishnan
Presented at the 29th Annual Technical Meeting of IIM held at Jamshedpur, Nov. 1975.
12. Preparation of crystal bar hafnium by the iodide process:
V.D. Shah, and C.M. Paul
Presented at the 29th Annual Technical Meeting of IIM held at Jamshedpur, Nov. 1975.
13. Fused salt electrorefining of zircaloy scrap:
J.C. Sehra, I.G. Sharma, P.L. Vijay, and A. Unnikrishnan
Presented at the 29th Annual Technical Meeting of IIM held at Jamshedpur, Nov. 1975.
14. Chlorination of rutile in fluidized beds:
P.L. Vijay, C. Subramanian, and Ch. Sridhar Rao
Presented at the 29th Annual Technical Meeting of IIM held at Jamshedpur, Nov. 1975.
15. Technology of titanium sponge production:
A.P. Kulkarni, Ch. Sridhar Rao, and C.V. Sundaram
Presented at the Seminar on 'Titanium Technology', held at Trivandrum, May 1975.
16. Production of titanium tetrachloride:
Ch. Sridhar Rao, and H.S. Ahluwalia
Presented at the Seminar on 'Titanium Technology', held at Trivandrum, May 1975.
17. Fused salt electrolysis for rare metal extraction and refining:
T.K. Mukherjee and C.K. Gupta
Presented at the Annual Technical Session of the Society for Advancement of Electrochemical Science and Technology on 'Fundamentals of Applied Electrochemistry' held at Bangalore, Nov. 1975.
18. Ultra purification techniques:
C.M. Paul and V.D. Shah
Presented at the Winter School in 'Chemistry and Metallurgy of Rare Metal Extraction', organised by Indian National Science Academy, held at Trombay, Jan. 1975.
19. Extractive Metallurgy of Beryllium:
C.M. Paul and K.S. Subbarao
Presented at the Winter School in 'Chemistry and Metallurgy of Rare Metal Extraction', organised by Indian National Science Academy, held at Trombay, Jan. 1975.

20. Some aspects of metallothermic and carbothermic reduction
C.K. Gupta
ibid
21. Refining of rare metals by molten salt electrolysis
C.K. Gupta
ibid
22. Preparation of hafnium metal by calciothermic reduction of hafnium oxide
I.G. Sharma, P.L. Vijay, J.C. Sehra, and C.V. Sundaram
BARC Report 828
23. Electrometallurgy of titanium, zirconium and hafnium
J.C. Sehra, I.G. Sharma and Ch. Sridhar Rao
Presented at the Symposium on 'Electrometallurgy' held at Cochin, May 1975, under the auspices of the Society for Advancement of Electrochemical Science & Technology
24. Halogenation processes in rare metal extraction
C.V. Sundaram and K.S. Subbarao
Presented at the Winter School in 'Chemistry and Metallurgy of Rare Metal Extraction', organised by Indian National Science Academy held at Trombay, Jan. 1975
25. Pyro-vacuum processes for extraction and refining of refractory metals
S.P. Garg and C.V. Sundaram
ibid
26. Internal friction studies on martensitic transformations in Zr-Mo and Zr-Ti alloys
S. Mishra and M.K. Asundi
Presented at the DAE Materials Science Symposium on 'Phase Transformations & Phase Equilibria' held at Indian Institute of Science, Bangalore, October 16-18, 1975.
27. Twinning in martensitic and ordering transformations
S. Banerjee, V. Seetharaman and R. Krishnan
ibid
28. Decomposition of the beta phase in a near eutectoid Zr-Cu alloy
P. Mukhopadhyay, S. Banerjee and R. Krishnan
ibid
29. Phase diagram studies in thorium-iron system
R.V. Patil and S.K. Khera
ibid

30. Influence of High Cooling Rates on the Growth of the Product in Liquid-Solid Transformations
P.K.K. Nayyar
ibid
31. Phase transformations in a hypo-eutectoid zirconium-copper alloy
P. Mukhopadhyay, S. Banerjee and R. Krishnan
Presented at the 29th Annual Technical Meeting of Indian Institute of Metals held at National Metallurgical Laboratory, Jamshedpur, November 14-17, 1975.
32. Interdiffusion studies in titanium-vanadium system
G.B. Kale, S.K. Khara and G.P. Tiwari
ibid
33. A computer programme for indexing selected area diffraction patterns from intermetallic compounds
S.K. Khara and P. Mukhopadhyay
ibid
34. Defect and defect cluster interactions with dislocations in zirconium
S. I. Ghosh and M.K. Asundi
ibid
35. Microstructural changes in rapidly quenched proeutectoid Al-Zn alloys
P.K.K. Nayyar and R.N. Tank
ibid
36. Defect structure and post irradiation annealing in neutron irradiated nickel base alloys
I.S. Ghosh, M.K. Maitra and B.D. Sharma
ibid
37. Deformation behaviour of nickel and nickel-1% titanium alloy below 0.5 T_m
M.K. Maitra, B.D. Sharma and P. Dasgupta -ibid-
38. Correlation effects in self-diffusion in Fe-Mn and Fe-Mo alloys
V.S. Raghurathan and B.D. Sharma -ibid -
39. Stress relaxation in zirconium and its alloys
P. Dasgupta
ibid
40. Dislocation-solute interaction and discontinuous yielding in solid solutions
V.V. Raman, C.N. Rao and M.K. Asundi
ibid

41. The effect of heat-treatment variables on the structure of the commercial Ti-3Al-1Mo-1V alloys
S.J. Vijayakar, S. Banerjee and R. Krishnan
ibid
42. Dislocation associated with hydride precipitates in zirconium-1% aluminium
V. Seetharaman, P. Mukhopadhyay and R. Krishnan
ibid
43. Consolidation and fabrication of rare metals
M.K. Asundi
Presented at the INSA-BARC Winter School in 'Chemistry and Metallurgy of Rare Metal Extraction' held at Trombay, Jan.13-30,1975
44. Titanium alloys - why and for whom?
V.S. Arunachalam and Dr.M.K. Asundi
Presented at the Titanium Conference held at Trivandrum, May 30-31, 1975
45. Metallurgical evaluation of explosion bonded materials
S. Banerjee, V. Seetharaman and M.K. Asundi
Presented at the Seminar on 'Shock Structure Interaction' at RRC, Madras, August 1975.
46. Serrated Yielding in Ni-1%Ti alloy
M.K. Matta, B.D. Sharma and P. Dasgupta
Communicated for publication.
47. Characterisation of UO₂ powders by radioactive adsorption
G.P. Tivari, N.C. Soni and S.V.K. Rao
Accepted for publication in Journal of Nuclear Materials.
48. A correlation of vacancy formation energy with cohesive energy
G.P. Tivari and R.V. Patil
Scripta Metallurgica, 2, 833, 1975
49. Studies in the corrosion of construction materials in the treatment of rock phosphate with H₂SO₄ : Part II : Corrosion of Nb, Ta and Ti alloys with Hf
P.R. Shihed and J. Balachandra
J. Electrochem. Soc. India 24 (1) 13 (1975)
50. Behaviour of titanium and its alloys with hafnium in selected corrosive media
P.R. Shihed and J. Balachandra
Anti corrosion, February 1975

51. Corrosion studies on Cu-Ni alloys and ferritic steel in salt water for desalination service
P.R. Shibad and J. Balachandra
BARC Report No.805
52. Preferential corrosion of epsilon martensite in austenitic stainless steel
P.K. De and K. Elayaperumal
Trans. Indian Institute of Metals, 28 (1975) 369
53. Corrosion Research in Progress - A contribution to the series in 'Corrosion' - MACE -
K. Elayaperumal
Corrosion 31 (June 1975) 226
54. Oxidation kinetics and hydrogen absorption of alloy of Zr with Nb and Cr
H.S. Gadiyar and J. Balachandra
Trans. IIM 28, 385 (1975)
55. Stress measurements and structural studies during the oxidation of Zr-base alloys
H.S. Gadiyar and J. Balachandra
Trans. IIM, 28, 391 (1975)
56. Stress corrosion cracking of Zr and Zircaloy-2 in Methanol/H₂O solution : Effect of applied stress
P.K. De and K. Elayaperumal
Presented at the 6th International Congress on Metallic Corrosion, Sydney, Australia, December 1975
57. Relation between the phase changes in the oxide and the transition phenomenon during the oxidation of Zr alloys
S.V. Phadnis and H.S. Gadiyar
Presented at the 6th Materials Science Symposium on 'Phase Transformations & Phase Equilibria' held at Bangalore, October 16-18, 1975
58. Oxidation of Zr-Ni alloys
S. Chakravarty and H.S. Gadiyar
Presented at the 29th Annual Technical Meeting of the IIM at Jamshedpur in November 1975
59. Some basic studies on corrosion of metals and alloys of interest to atomic energy programmes
K. Elayaperumal and H.S. Gadiyar
Delivered at the Symposium on Fundamentals of Applied Electrochemistry, organised by SAEEST, held at Bangalore, November 8-9, 1975

60. **Electrochemical measurements of aqueous corrosion processes of inconel 600 at high temperature and pressure**
P.K. De
ibid
61. **Electrochemical extraction and deposition of some less common metals**
Delivered at the Silver Jubilee symposium on "applications of electrochemistry", organised by the Electrochemical Society of India, held at Bangalore, 16-17 August, 1975
62. **Electrowinning of rare earth metals**
Sohan Singh and J. Salschandra
Presented at the Symposium on Electrometallurgy on 8-9 May 1975 at Ernakulam, Cochin
63. **Reaction sintering of uranium monocarbide**
B.D. Zope and V.K. Moorthy
Presented at the 39th Annual Technical Meeting of the Ind. Cer. Soc. March 1975, Bombay
64. **Sintering of Beryllium Oxide - Influence of furnace atmosphere and minor addition on different beryllia powders**
R. Bhat and V.K. Moorthy
ibid
65. **Factors influencing sinterability of pure oxides - Study of development of morphology in magnesia powders**
C.M. Pathak and V.K. Moorthy
ibid
66. **A study on the degree of crystallinity of magnesia powders from magnesium hydroxide**
G. Eswara Prasad and V.K. Moorthy
ibid
67. **In-situ hot stage electron microscope study on the sintering of magnesia derived from magnesium hydroxide**
G. Eswara Prasad and V.K. Moorthy
ibid
68. **Influence of calcination treatment and firing atmosphere on dielectric properties of barium titanate**
A.K. Nulkarai, D.D. Upadhyaya and V.K. Moorthy
ibid

69. Studies on sintering of barium titanate - Part I -
Influence of calcination and sintering treatments on
dielectric properties
K. Thiagarajan and V.K. Moorthy
ibid
70. Reaction sintering of uranium monocarbide
B.D. Zope and V.K. Moorthy
Trans. Ind. Cer. Soc. 73(3) (1975)

